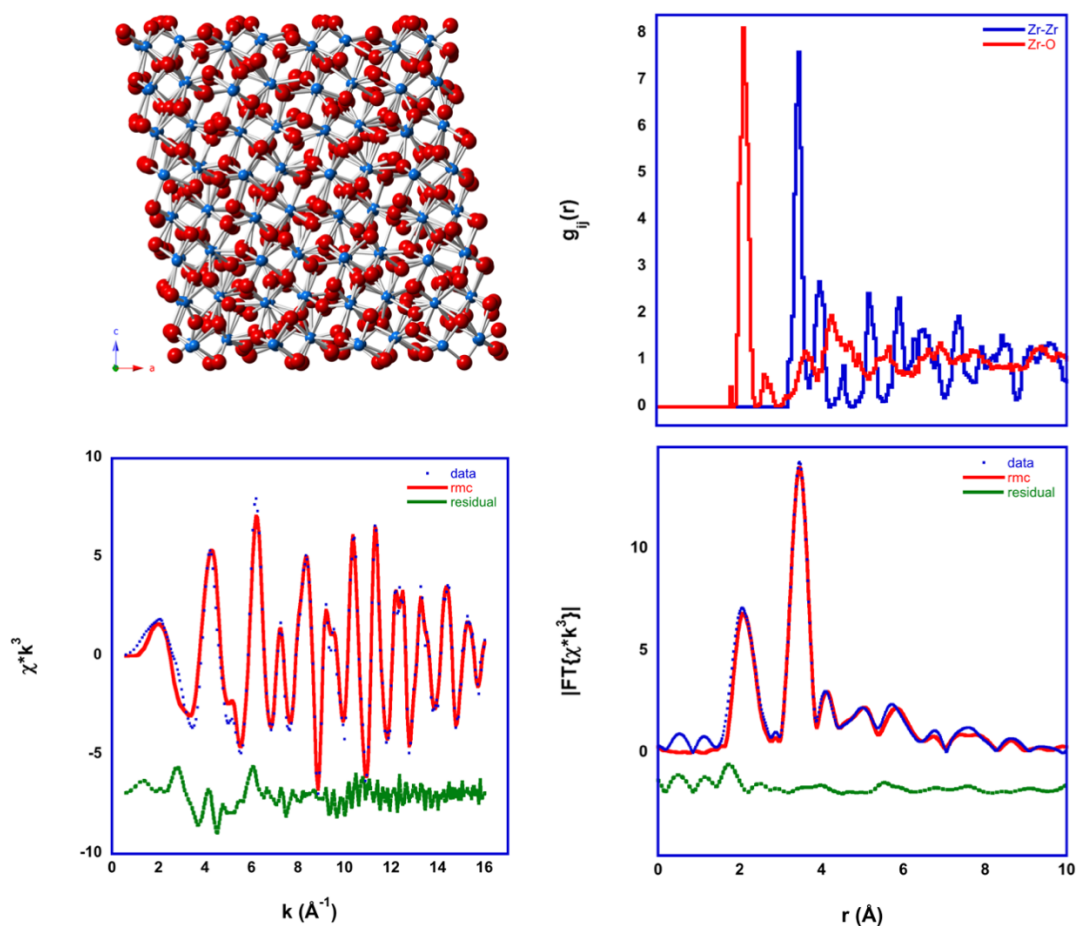


rmcxas

A program to perform Reverse Monte Carlo (RMC) analysis of Extended X-ray absorption Fine Structure Spectra and X-ray, neutron or electron scattering or diffraction

— Manual —



Markus Winterer

Duisburg, 04/16/2025

Contents	i
Foreword and Acknowledgement	iii
Code Availability	iii
1 Introduction	1
2 Theoretical Background	1
1 Reverse Monte Carlo (RMC) analysis	1
2 EXAFS	1
3 EXAFS – complex systems	2
4 EXAFS – low frequency signal	3
5 Scattering – Structure factor	4
6 Scattering – Debye scattering equation	5
7 Scattering – Background signal	6
8 Scattering and diffraction – atomic form factors	6
9 Diffraction – Rietveld refinement	7
10 Coupling Rietveld refinement and RMC of EXAFS	10
11 Optimization algorithm for Rietveld and background refinement	13
3 Methodology	14
1 Information required	14
2 Procedure (flow of RMC analysis process)	16
3 Limits of the code and hints for using it	16
4 File type when using rmcxas	17
5 Control files	17
6 Input files	24
7 Output files	28
4 References	31
5 Publications related to rmcxas	33
5 Appendices	35
1 Conversion between descriptors of phase composition	35
2 Files to perform rmcxas	35
3 Auxiliary files	37
6 Examples	40
1 RMC of one EXAFS spectrum: m-ZrO ₂	40
2 Rietveld refinement of one XRD data set: m-ZrO ₂	43
3 Coupled RMC of EXAFS and Rietveld of XRD: m-ZrO ₂	47
4 Coupled RMC of EXAFS and Rietveld of XRD: Al doped t-ZrO ₂	49
5 Coupled RMC of EXAFS and Rietveld of XRD for two phases: m- und t-ZrO ₂	51
6 Coupled RMC of EXAFS and Rietveld of XRD and neutron diffraction: m-ZrO ₂	52
7 Simultaneous RMC of EXAFS and neutron scattering $S(q)$: m-ZrO ₂	53
8 Simultaneous RMC of Co and Fe K-edge EXAFS: Co doped ZnO	54
9 Simultaneous RMC of Co and Fe K-edge EXAFS: CoFe ₂ O ₄	55
10 Simultaneous RMC of EXAFS and scattering via DSE: SnO ₂	56

Foreword and Acknowledgements

The original motivation of the development of the data analysis tool presented here was to obtain information about the atomistic structure of highly disordered materials, especially glasses and nanomaterials from EXAFS spectra, beginning in 1985 during my doctoral studies. Since 1996 I developed then `rmcxas` as a side project without direct funding.

However, I very gratefully acknowledge the financial support in all these years by the following funding agencies either through fellowships, projects or beamtime at synchrotron and neutron radiation facilities: Alexander von Humboldt foundation, Argonne National Laboratory (Department of Energy, US), DESY (Helmholtz Association HGF), Daresbury (Council for the Central Laboratory of the Research Councils, UK), NFL Studsvik (Sweden), the European Commission and especially the Deutsche Forschungsgemeinschaft (DFG, German Research Foundation).

I am very thankful to Tomas Diaz de la Rubia and Maria-Jose Caturla (both then at the LLNL) who introduced me to molecular dynamics which became an important root to the `rmcxas` code. I also want to thank all the people who supported me and my group at beamlines of synchrotron and neutron radiation facilities. They helped us to obtain high quality data which allow the type of data analysis described here and to obtain information about the atomistic structure of complex materials which are otherwise difficult or impossible to extract (in chronological order): first of all Ronald Frahm who introduced me to EXAFS at HASYLAB, Lennox Iton (ANL) who inspired me to perform EXAFS experiments and data analysis, Farrel Lytle (Boeing) who taught me the roots of EXAFS, Lynne Soderholm (ANL) who shared some of her beamtime initiating my EXAFS experience at BNL, Larc Tröger (HASYLAB@DESY), Edmund Welter (HASYLAB@DESY and PETRA@DESY), Adam Webb (HASYLAB@DESY), Klaus Attenkofer (HASYLAB@DESY, APS@ANL), Andy Dent, Fred Mosselmans and Menno Oversluizen (all at Daresbury), Robert McGreevy and Bob Delaplane (both the at NFL Studsvik), Winfried Frentrup (BESSY), Chun Loong (IPNS@ANL), Jim Richardson (IPNS@ANL), Martin Etter (PETRA@DESY), Sungsik Lee (APS@ANL) and Chengjun Sun (APS@ANL).

I am also indebted to my coworkers at TU Darmstadt and University Duisburg-Essen and collaborators who inspired me to develop and improve the code, provided me with materials and performed the measurements and data analysis together with me (in chronological order): Robert Nitsche, Klaus Neubeck, Sylke Klein, Stefan Seifried, In-Kyum Lee, Andreas Benker, Andreas Möller, Joachim Brehm, Yong Sang Cho, Johannes Seydel, Herman Sieger, Kranthi Kumar, Thorsten Enz, Sabari Bhattacharya, Francois Farges, Alexander Kompch, Udo Dörfler, Gerd Bacher, Moazzam Ali, Christian Notthoff, Alice Sandmann, Lukas Helmbrecht, Ruzica Djenadic, Martin Busch, Carolin Schilling, Viktor Mackert, Julia Gebauer, Karel Maca, Janusz Fidelus, Einar Kruis, Wayne Gladfelter, David Norris, Martin Muhler, Alexander Levish, Jeldrik Schulte, Shradha Joshi, Martin Schroer, and especially Vladimir Srdic with whom I generated the zirconia based materials and Stevan Ognjanovic, Sasa Lukic and Jeremias Geiss for the SnO_2 and CoFe_2O_4 samples used as examples in chapter 6.

Code Availability

The `rmcxas` code described here and developed by the author is available for linux and Apple computers on: <https://www.rmcxas.de>

1 Introduction

rmcxas is a program to perform Reverse Monte Carlo (RMC) analysis of Extended X-ray absorption Fine Structure (EXAFS) spectra and X-ray, neutron or electron scattering or diffraction data to obtain quantitative information about the structure of materials. **rmcxas** has been developed since 1996, initially to analyze EXAFS data of disordered systems like glasses and nanoparticles (Winterer 2000).

Structure may be defined as the geometric arrangement of elementary building blocks in an object, here a material. In the context of data analysis of extended X-ray absorption spectra or (wide angle) X-ray, neutron or electron scattering, elementary building blocks are atoms or groups of atoms. Investigating structure from spectroscopy or scattering means to extract information about real (direct) space from reciprocal space data. In case of reverse Monte Carlo simulations the solution to this inverse problem is the data analysis based on the refinement of a model which consists of an atom configuration (a simulation box containing typically of the order of 1000 to 10.000 atoms). Therefore, RMC data analysis is intrinsically not model free. However, different physical models can be tested and refined.

2 Theoretical Background of RMC (Winterer 2002)

2.1 Reverse Monte Carlo (RMC) analysis

Reverse Monte Carlo (RMC) simulations are based on the Metropolis Monte Carlo (MC) algorithm (Allen and Tildesley 1987) where the interatomic potential is replaced by the difference between experimental data, i. e. scattering intensity and / or EXAFS spectra, and simulations based on an atomic configuration (McGreevy and Pusztai 1988). MC steps randomly move an atom in the configuration from which a new simulation is computed. MC steps are always accepted when the difference between experimental and computed data gets smaller. Otherwise, they are accepted with a probability of

$$p = \exp\{-\Delta\beta\} \quad (1)$$

with (Gurmann and McGreevy 1990)

$$\beta = \frac{\sum_i [k_i^n (d_i - s_i)]^2}{\sum_i [\sigma_i \cdot k_i^n \cdot d_i]^2} \quad (2)$$

where d_i are the experimental data, s_i are the simulated data obtained from the atomic configuration, k_i^n is a weighting of data in case of EXAFS with k as photoelectron wave vector and σ_i is an error estimate for the data which replaces the ‘temperature’ in Metropolis MC simulations. The fitting index R is defined as

$$R(\%) = 100 \cdot \frac{\sum_i |d_i - m_i|}{\sum_i |d_i|} \quad (3)$$

which corresponds to the ‘pattern’ R -value (R_p) in Rietveld refinements (Young 1995).

2.2 EXAFS

rmcxas was initially coded for the analysis of EXAFS spectra. EXAFS spectra (single scattering contribution) may be computed from partial pair distribution functions (pPDFs, $g_{ij}(r)$) by integration over the product of the pPDFs and the EXAFS kernel $\gamma_{ij}(k, r)$ for the corresponding absorber-scatterer pair ij (Filipponi 1994):

$$\chi_i(k) = \sum_j 4\pi n_j \int g_{ij}(r) \cdot \gamma_{ij}(r, k) \cdot r^2 dr \quad (4)$$

where

$$k = \frac{1}{\hbar} \left(2m(E - E_0) \right)^{\frac{1}{2}} \quad (5)$$

is the photoelectron wave vector computed from the X-ray photon energy E and the energy of the absorption edge E_0 and the EXAFS kernel (Filipponi 1994)

$$\gamma_{ij}(r, k) = A_{ij}(r, k) \cdot \sin\{2kr_{ij} + \phi_{ij}(r, k)\} \quad (6)$$

is an amplitude and phase modulated harmonic function. EXAFS amplitude $A(r, k)$ and phase $\phi(r, k)$ functions are taken from ab initio feff simulations (Rehr et al. 2010) using the initial atom configuration. The pPDFs are defined by the number of atoms j at a distance r from atom i

$$g_{ij}(r) = \frac{n_{ij}(r)}{n_j} \quad (7)$$

divided by the average number density of the neighboring atom j

$$n_j = \frac{N_j}{V} \quad (8)$$

The code uses implicitly periodic boundary conditions.

Initial applications of the code are published in Winterer 2000 and 2002 and Winterer et al. 2002.

2.3 EXAFS – complex systems (Geiss et al. 2022)

The analysis of complex samples, especially complex oxides like spinels or perovskites and phase mixtures is enabled in the code. Multiple sites of identical elements for absorber atoms contribute to a single spectrum and may occur

- homogeneously for example as $\text{Fe}^{2+} / \text{Fe}^{3+}$ or Fe_{tet} , Fe_{oct} in Fe_3O_4
- heterogeneously as in multiple phases like $(\text{Fe}_2\text{O}_3 + \text{FeO} + \text{Fe})$ or at surfaces/interfaces and cores of nanoparticles.

Therefore, the equation to compute EXAFS (3) is modified to

$$\chi_i(k) = \sum_{i \text{ of } I} w_i \sum_j 4\pi \rho_j \int g_{ij}(r) \cdot \gamma_{ij}(r, k) \cdot r^2 dr \quad (9)$$

where w_i contains phase fraction and relative atomic fraction of absorber sites i contributing to spectrum I , ρ_j is the number density of scatterer j , g_{ij} the partial pair distribution function, γ_{ij} the EXAFS kernel and r the interatomic distance. The integral is performed as sum over all bins of g_{ij} .

Multiple sites typically mean a large number of different atom types and, therefore, a large number of partial pair distribution functions, pPDF, $g_{ij}(r)$. Since in EXAFS typically not all scatterers are also measured as absorbers the matrix of the pPDFs is holey and if many absorbers in different phases contribute an elaborate assignment scheme has to be used to ensure correct computation (Fig. 1).

Each atom – even of the same chemical element – is considered an individual type of atom if it is in a different chemical state (oxidation state, coordination, phase). Each different atom is identified by a unique identifier, the atom type number i .

2.4 EXAFS – low frequency signal

Extended X-ray absorption fine structure (EXAFS) spectra are often obscured by a low frequency signal (LFS). The LFS may originate for example from Atomic X-ray Absorption Fine Structure (AXAFS) first identified by Holland et al. (1978). According to Rehr et al. (1994) AXAFS is an oscillatory contribution to the XAFS background signal which originates in the scattering of the outgoing photoelectron wave within the absorber atom. Multielectron excitations are another explanation provided for example by Filipponi et al. (1988) and D'Angelo et al. (1993). They are caused by strong electron-electron interaction within the absorbing atom. Simultaneous refinement in Reverse Monte Carlo simulations using an empirical EXAFS like expression for LFS and a structural model for EXAFS allows the separation of both signals. An empirical expression for LFS is used to fit the residual (EXAFS data minus rmc fit) and allows to extract LFS without disturbing the EXAFS signal. The expression is analogous to the standard parametrization of the EXAFS signal (Teo 1986, Teo et al. 1977 and Lee et al. 1977):

$$\chi_{\text{lfs}}(k) = A_{\text{lfs}}(k) \cdot \sin(\phi_{\text{lfs}}(k)) \quad (10)$$

									$j_{\text{scat}} \rightarrow$
$I = 1$	1	2	3	4	0	0	0	0	0
	2	5	6	7	0	0	0	0	0
	3	6	8	9	0	0	0	0	0
	4	7	9	10	0	0	0	0	0
$I = 1$	0	0	0	0	11	12	0	0	0
	0	0	0	0	12	13	0	0	0
	0	0	0	0	0	0	14	15	16
$I = 1$	0	0	0	0	0	0	15	17	18
$i_{\text{abs}} \downarrow$	0	0	0	0	0	0	16	18	19

phase 1
phase 2
phase 3

Fig. 1: Matrix of pPDF labels for multiple absorber sites for a hypothetical example with a total number of 9 scatterers in 3 phases to which 19 independent pPDFs are assigned.

$$A_{\text{ifs}}(k) = \frac{a_0}{k \cdot b_1^2} \cdot \exp\{-2a_1b_1\} \cdot \exp\{-2a_2^2k^2\} \quad (11)$$

$$\phi_{\text{ifs}}(k) = b_0 + 2b_1k + b_2k^2 \quad (12)$$

using a minimum number of parameters. More / higher order terms, for example corresponding to third or fourth cumulant, replacement of a_0 in A_{ifs} by a Lorentzian term or adding a b_3/k^3 term in ϕ_{ifs} are possible. However, values of these extra parameters are typically smaller than the estimated error and, therefore, insignificant or make the fit instable. Another extension would be the introduction of additional LFS contributions.

2.5 Scattering – Structure Factor (Winterer et al. 2002)

For isotropic samples, we may also use the pPDFs to compute the scattering intensity via the structure factor (see for example Cusack 1987)

$$I(q) \propto \langle f^2 \rangle - \langle f \rangle^2 + \langle f \rangle^2 \cdot F(q) \quad (13)$$

where

$$q = \frac{4\pi \sin \theta}{\lambda} \quad (14)$$

is the scattering vector,

$$F(q) = \sum_i^N \sum_{j=i}^N \left(\gamma_{ij} (S_{ij}(q) - 1) \right) \quad (15)$$

is the total structure factor,

$$\langle f^2 \rangle = \sum_i n_i f_i^2 \quad (16)$$

is the weighted average of the squared atomic form factors and

$$\langle f \rangle^2 = \left(\sum_i n_i f_i \right)^2 \quad (17)$$

is the squared average of the weighted atomic form factors where the atomic form factors

$$f_i = f_i(q) \quad (18)$$

are depending on the scattering vector for X-ray and electron scattering. Using the coefficient

$$\gamma_{ij} = \frac{n_i n_j f_i f_j}{\langle f \rangle^2} \quad (19)$$

we can compute the total structure factor $F(q)$ from the partial structure factors

$$S_{ij}(q) = 1 + 4\pi \int_0^\infty r^2 (g_{ij}(r) - 1) \frac{\sin\{q \cdot r\}}{q \cdot r} dr \quad (20)$$

by integration over the product of $(g_{ij}(r) - 1)$ and the sinc-Function of $q \cdot r$.

Obviously, the pPDFs are the key element in RMC. They contain the relevant quantitative structural information regarding

- coordination number (proportional to the area under a peak)
- mean coordination distance (position of a peak), and
- root mean square displacement (width of a peak)

which can be extracted by moment analysis of the distributions including higher moments.

2.6 Scattering – Debye-Scattering Equation (Winterer and Geiß 2023)

In principle, we can use a mutual physical model to compute EXAFS spectra and X-ray scattering data as described. However, in the derivation of this structure factor $S_{ij}(q)$, it is assumed that the system is infinitely large, which is certainly not a good model for small nanoparticles. This assumption is used to separate the forward scattering and results in the term $(g_{ij}(r) - 1)$ in the (partial) structure factor (eq. 20).

The scattering intensity for isotropic samples may alternatively also be computed using the Debye scattering equation (DSE) instead of the structure factor:

$$I(q) \propto \sum_i \sum_j f_i \cdot f_j \frac{\sin\{q \cdot r_{ij}\}}{q \cdot r_{ij}} \quad (21)$$

However, a direct implementation of the DSE is computationally too expensive for refinement of experimental data. Realizing that the nominator in the definition of the pPDFs

$$n_{ij}(r) = n_j \cdot g_{ij}(r) \quad (22)$$

is the number of atoms of type j at a distance r from atom type i , we can use this information to compute the scattering intensity from a binned version of the DSE from $g_{ij}(r)$ efficiently:

$$I(q) \propto \sum_l \sum_{ij} n_i \cdot n_{ijl} \cdot f_i \cdot f_j \frac{\sin\{q \cdot r_l\}}{q \cdot r_l} \Delta V_l \quad (23)$$

with the binned number of atom pairs

$$n_{ijl} = n_{ij}(r) \quad (24)$$

and the volume of a spherical shell of the width of a bin

$$\Delta V_l = \frac{4}{3} \pi (r_{l+1}^3 - r_l^3) \quad (25)$$

where l is the bin number assigned to the distance r_l in the binned pair distribution function.

This approach is only reasonable for small nanocrystals with diameters below about 10 nm. For larger coherent diffracting domain sizes the periodicity of the crystalline structure (translational symmetry) needs to be exploited such as in Rietveld refinement.

Scattering is computed either by computing a binned Debye scattering equation (eq. 23) for cluster models or the scattering structure factor (eqs. 15 and 20) and scattering intensities (eq. 13) for periodic models based on the partial pair distribution functions g_{ij} generated from a mutual structural model (atomic configuration) which are also used to compute EXAFS (eq. 4). For scattering all partial pair distribution functions and larger distances are required. Atomic form factor functions as a function of q are computed first before the Monte Carlo steps.

2.7 Scattering – background signal

Additionally, the amplitude A of the scattering signal and scattering background $B(q)$

$$I(q) = A \cdot \sum_i \sum_j f_i \cdot f_j \frac{\sin\{q \cdot r_{ij}\}}{q \cdot r_{ij}} + B(q) \quad \text{or} \quad I(q) = A \cdot \left(\langle f^2 \rangle - \langle f \rangle^2 + \langle f \rangle^2 \cdot F(q) \right) + B(q) \quad (26)$$

have to be adjusted. For the background $B(q)$ function 6 of GSAS (Larson and Dreele 2004, p. 130) is used as it provides stiff polynomial allowing to fit the background for X-ray and neutron scattering without fitting the structural part of the signal:

$$B(q) = b_1 + \frac{b_2}{1} \cdot q^2 + \frac{b_4}{2} \cdot q^4 + \frac{b_6}{6} \cdot q^6 + \frac{b_3}{1} \cdot q^{-3} + \frac{b_5}{2} \cdot q^{-4} + \frac{b_7}{6} \cdot q^{-6} \quad (27)$$

Amplitude and background are fit by adjusting the coefficients A and b_i using a Monte Carlo algorithm once at the beginning of every RMC cycle. The same amplitude and background function is used for the structure factor $F(q)$ to be able to adjust scale and offset. In case of optimal conversion of raw scattering data to structure factor this should not be necessary.

2.8 Scattering and Diffraction – atomic form factors

The atom form factors f_j depend on the type of diffraction probe (X-rays, electrons or neutrons) and in case of X-rays and electrons on the scattering angle which is computed from the Cromer-Mann coefficients ($a_1, b_1, a_2, b_2, a_3, b_3, a_4, b_4, c$) for X-rays (for example from Maslen et al. 2006) and electrons:

$$f_j(q_K) = c + \sum_{l=1}^4 a_l \cdot \exp\{-b_l \cdot s_K\} \quad \text{with} \quad s_K = \frac{q_K^2}{16\pi^2} \quad (28)$$

In case of neutrons a single constant (c) per isotope (or isotope mixture) is used.

2.9 Diffraction – Rietveld refinement (Winterer 2002 after Young 1995)

In Rietveld analysis the complete intensity profile $I(2\theta)$ or $I(q)$ of the powder diffraction pattern is refined by non-linear least square fitting of a structural (crystallographic) model simultaneously with instrumental and other specimen parameters (microstructural parameters, e.g.):

$$I_{\text{Rietveld}}(2\theta) = b(2\theta) + s \sum_p \frac{v_p}{V_p^2} \sum_K L_K |F_K|^2 \phi(2\theta_i - 2\theta_K) P_K A_K, \quad \sum_p v_p = 1 \quad (29)$$

where $b(2\theta)$ is the background intensity (thermal diffuse or disorder scattering, see e.g. Richardson 1995), s is a scale factor, v_p the volume fraction and V_p the unit cell volume of phase p , L_K contains the Lorentz, polarization and multiplicity factors, ϕ is the profile function, P_K is the preferred orientation function, A_K is the absorption factor and F_K is the structure factor. The index K represents the Miller indices for the Bragg reflections.

The background is fitted using a polynomial function (Young 1995):

$$B(2\theta_i) = b_0 + \sum_{m=2}^{12} b_m \cdot \left(\frac{2\theta_i}{b_p} - 1 \right)^{m-1} \quad (30)$$

Preferred orientation function P_K and absorption A_K are set to 1 and the Lorentz-, and polarization-correction is computed according to

$$L_K = \frac{1 + \cos^2(2\theta_K)}{\sin^2(\theta_K) \cos(\theta_K)} \text{ for XRD or } L_K = \frac{1}{\sin^2(\theta_K) \cos(\theta_K)} \text{ for neutron diffraction} \quad (31)$$

(Pecharsky and Zavalij 2009).

In a first step the positions of the Bragg reflections are computed for each phase p and output to `latdis.dat.p`. The code computes the maximum possible Miller index for the wavelength used from which all d_K -values are computed using the formula for the triclinic crystal system and the lattice constants provided.

For crystalline materials the translational symmetry can be exploited to reduce the summation in the structure factor to the atoms in the unit cell which is computed in the second step:

$$F_K = \sum_j N_j f_j \exp\{2\pi i(hx_j + ky_j + lz_j)\} \exp\{-M_j\} \quad (32)$$

where N_j is the occupancy of the site j . Miller indices are labeled as h, k, l and x_j, y_j, z_j are the position parameters of the j th atom in the *unit cell*. The scattering vector for each Bragg reflection of index K is

$$q_K = \frac{4\pi \sin \theta_K}{\lambda} \quad (33)$$

M_j is the temperature factor:

$$M_j = \frac{B_j \cdot \sin^2 \theta_K}{\lambda^2}, \quad B_j = 8\pi^2 \langle u_j^2 \rangle \quad (34)$$

where $\langle u_j^2 \rangle$ is the root-mean-square displacement of the j th atom parallel to the diffraction vector which is apparent from

$$\langle u_j^2 \rangle = \langle (\bar{u}_j \cdot \bar{q})^2 \rangle \quad (35)$$

Degenerate reflections are combined and all reflections are rebinned to a bin width of $0.001^\circ 2\theta$. Reflections with a scattering amplitude below 0.01% of the maximum scattering amplitude are neglected. The remaining Bragg reflections are convoluted with a modified Thompson-Cox-Hastings pseudo-Voigt profile function (Young 1995):

$$\phi = \eta \cdot L + (1 - \eta) \cdot G \quad (36)$$

where L and G are Lorentzian and Gaussian profiles:

$$L = \frac{\frac{2}{\pi \Gamma_K}}{1 + \frac{4(2\theta_i - 2\theta_K)^2}{\Gamma_K^2}} \quad (37)$$

$$G = \left(\frac{4 \ln 2}{\pi \Gamma_K^2} \right)^{\frac{1}{2}} \exp \left\{ - \frac{4 \ln 2 \cdot (2\theta_i - 2\theta_K)^2}{\Gamma_K^2} \right\} \quad (38)$$

$2\theta_i$ are the values of the independent variable of the measurement, $2\theta_K$ are the positions of the Bragg reflections, η is a mixing factor depending on the contribution of size and microstrain to the width of the diffraction peaks which cause the line broadening Γ_K :

$$\eta = 1.36603q - 0.47719q^2 + 0.1116q^3, \quad q = \frac{\Gamma_L}{\Gamma} \quad (39)$$

$$\Gamma = \left(\Gamma_G^5 + A\Gamma_G^4\Gamma_L^1 + B\Gamma_G^3\Gamma_L^2 + C\Gamma_G^2\Gamma_L^3 + D\Gamma_G^1\Gamma_L^4 + \Gamma_L^5 \right)^{0.2} \quad (40)$$

with the coefficients $A = 2.69269$, $B = 2.42843$, $C = 4.47163$, $D = 0.07842$ and the Lorentzian and Gaussian contribution to the full width at half maximum:

$$\Gamma_L = X \tan \theta + \frac{Y}{\cos \theta} \quad (41)$$

$$\Gamma_G = \left(U \tan^2 \theta + V \tan \theta + W + \frac{Z}{\cos^2 \theta} \right)^{\frac{1}{2}} \quad (42)$$

The Cagliotti parameters U , V , and W are used as instrumental broadening parameters. The isotropic Lorentzian component for size d and microstrain ε are Y and X whereas the Gaussian components are $Z^{1/2}$ and $U^{1/2}$ respectively (Balzar et al. 2004).

First, the parameters d and ε are converted to degrees

$$E = \frac{180}{\pi} \varepsilon \quad (43)$$

$$D = \frac{180}{\pi} \frac{\lambda}{d} \quad (44)$$

Since the full width at half maximum, FWHM (Γ), in the profile function is not identical to the integral breadth β of a Bragg reflection, the conversion of microstrain $\varepsilon(-)$ and volume weighted domain size d (Å) needs to be converted according to

$$\Gamma_L = \frac{2}{\pi} \beta_L \quad (45)$$

for Lorentzian contributions and

$$\Gamma_G^2 = \frac{4 \cdot \ln(2)}{\pi} \beta_G^2 \quad (46)$$

for Gaussian contributions. Therefore,

$$X = \frac{2}{\pi} E \quad (47)$$

$$Y = \frac{2}{\pi} D \quad (48)$$

and

$$U = \frac{4 \ln(2)}{\pi} E^2 + U_{\text{inst}} \quad (48)$$

$$V = V_{\text{inst}} \quad (50)$$

$$W = W_{\text{inst}} \quad (51)$$

$$Z = \frac{4 \ln(2)}{\pi} D^2 \quad (52)$$

where the wavelength and the particle size (volume weighted) are in units of Å.

The volume fraction of a phase k can be converted to the molar fraction according to

$$x_k = \frac{\rho_k v_k}{\sum_k \rho_k v_k} \quad (53)$$

(see appendix) using the number densities ρ_k .

Additionally, systematic variations in the independent variable (2θ , resp. q) are corrected by refining

$$2\theta_{\text{corr}} = 2\theta + t_0 + t_s \cdot \cos(\theta) + t_t \cdot \sin(2\theta) \quad (54)$$

with zero offset t_0 , sample shift t_s , and sample transparency t_t as parameters.

For nonmonochromatic laboratory X-ray sources (K_{α} -radiation of Cr, Mn, Fe, Co, Ni, Cu, Mo, Ag, W, and Au indicated by negative wavelength in `rmc.par`), the corresponding wavelengths are tabulated in code) two diffractograms are added for $K_{\alpha 1}$ and $K_{\alpha 2}$) with an intensity ratio of 2:1 (Hölzer et al. 1997). Up to 3 diffractograms may be refined simultaneously.

2.10 Coupling Rietveld refinement and RMC of EXAFS (Winterer 2025)

It is possible to couple both RMC refinement of EXAFS data and Rietveld refinement of diffraction data by mapping structural parameters consistently (Fig. 2). In order to do this Rietveld refinement is performed using only translational symmetry to describe the periodic crystal structure without point symmetry (in space group P1). We call this ‘P1-Rietveld refinement’.

Rietveld parameters which may be coupled to EXAFS refinement (`ucc2coo` subroutine, see Fig. 3) are:

- lattice constants: $a, b, c, \alpha, \beta, \gamma$ by updating the metric matrix,
- occupation number and fractional coordinates of sites (o, u, v, w) by generating new atom configurations after each Rietveld refinement. The occupation number allows vacancies (< 1.0) and substitution (using identical fractional coordinates with a different atom type).
- phase fraction: v

RMC refinement of EXAFS results which may be coupled to Rietveld (`coo2ucc` subroutine, see Fig. 2, 3, and 4) are:

- fractional coordinates of sites: u, v, w by ‘distilling’ atom positions in the RMC atom configuration back to the unit cell,
- Debye-Waller factors (mean square displacements, $\langle u^2 \rangle$) by computing the mean square displacement of atoms relative to the average, ‘distilled’ position,
- microstrain: ε by computing the relative displacement from reference positions of the previous Rietveld refinement cycle

Coupling levels (parameter in `rmc.par`):

- 0 no coupling except in the initial simulation when the crystallographic parameters are used to generate the atom configurations for RMC refinement of EXAFS data (separate, parallel refinement)
- 1 coupling Rietveld refinement results to EXAFS
- 2 coupling level 1 plus coupling of EXAFS results to Rietveld
- 3 coupling level 2 plus transferring Debye-Waller factor from Rietveld to EXAFS

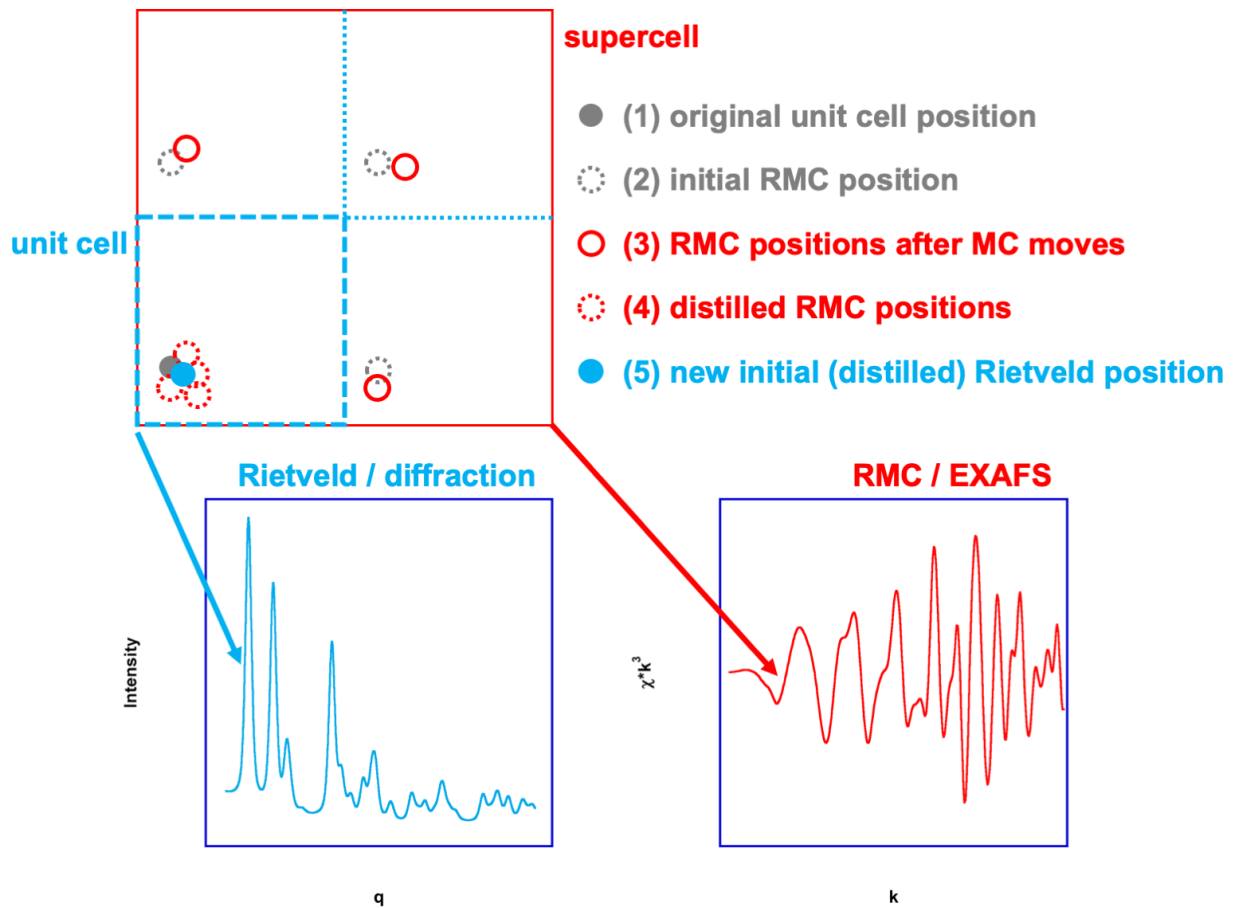


Fig. 2: Scheme of coupling between Rietveld refinement of diffraction data and RMC analysis of EXAFS spectra: one cycle of a feedback loop consists of the steps (1) initial atom position in unit cell (obtained by Rietveld refinement, solid grey circle) (2) expansion into supercell (dotted grey circles), (3) RMC moves for EXAFS analysis (red circles), (4) destillation of RMC supercell back into unit cell (red dotted circles) and (5) generation of new initial (average) atom positions (solid blue circle) for the next cycle in the feedback loop starting with Rietveld refinement.

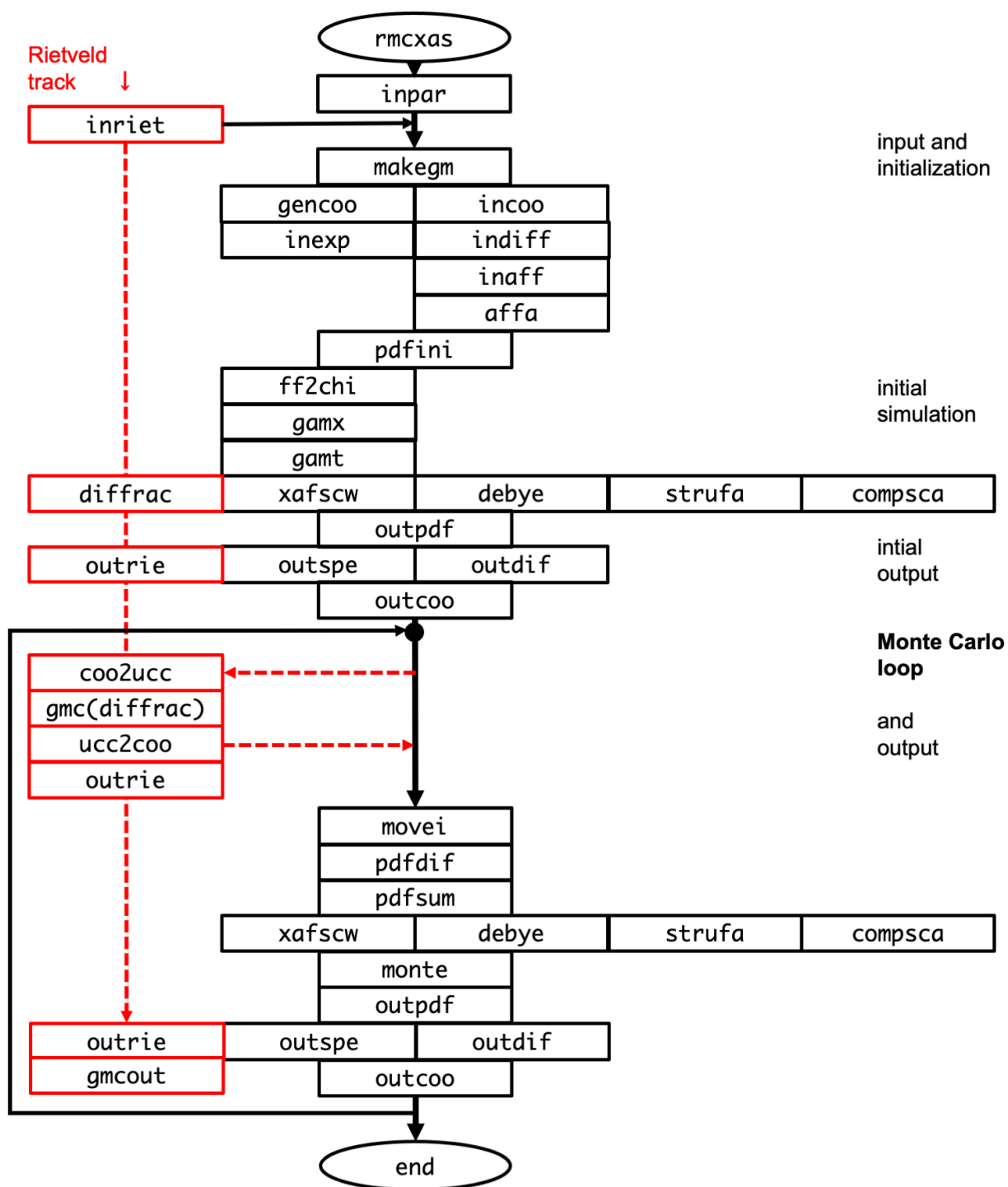


Fig. 3: Flowchart of the `rmcxas` code including Rietveld refinement (red). The Rietveld track has a separate Monte Carlo loop within `gmc` and uses `diffrac` to compute the Rietveld diffractogram.

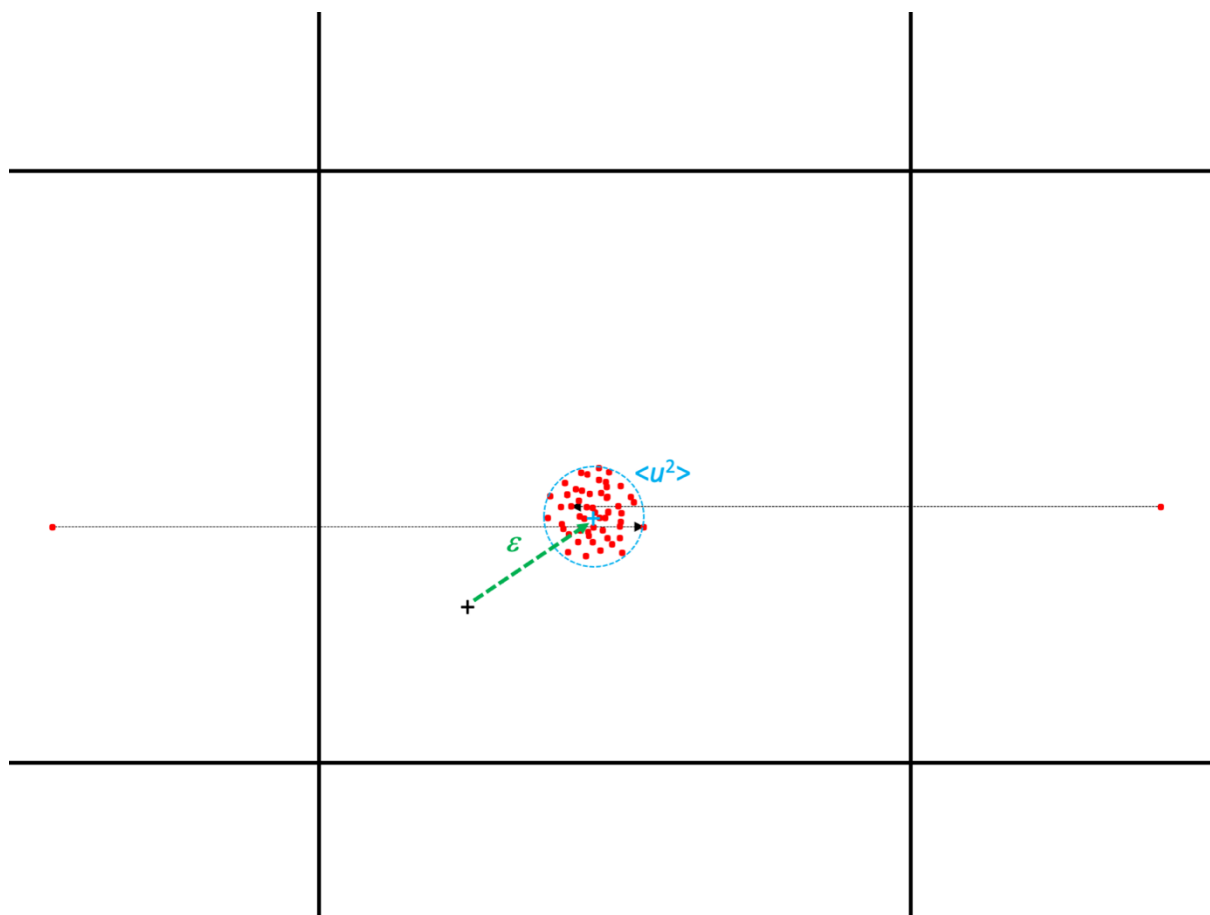


Fig. 4: ‘Distilling’ MC atom coordinates back to a single unit cell as indicated by black arrows and determination of microstrain and mean square displacement estimates from the distilled coordinates. The black cross indicates the (average) atom position after Rietveld refinement (obeying translational symmetry), the red cloud of dots represents the distribution generated by MC moves. The difference between Rietveld position and average MC position is used to estimate the microstrain and the distribution of the cloud of red points (distilled MC atom coordinates) from the average position (blue cross) is used as a measure for the Debye-Waller factor (the schematic drawing exaggerates the atom distribution and movement for clarity).

2.11 Optimization algorithm for Rietveld and background refinement

The optimization algorithm for Rietveld and background refinement (for EXAFS and scattering data) uses an MC code with adaptive step size according to Allen and Tildesley (1987).

The RMC code to analyse EXAFS data does not use adaptive step size.

3 Methodology

3.1 Information required before performing refinement using rmcxas

- At least one data set (EXAFS or scattering: any file name up to 31 characters long)
- Information to generate the EXAFS kernels (from feff: feffijkl.dat file) and / or atom form factors for scattering / diffraction (Cromer-Mann coefficients: rmc.aff.i file)
- A structural model either based on a unit cell (fractional coordinates: rmc.ucc.i file) or a simulation box (cartesian coordinates: rmc.coo.i file). This information typically comes from Rietveld refinement of diffraction data of your sample. It may also be the output of a DFT, MD or MC simulation, from original publications or crystallographic data bases like ICSD or COD.

The structure around each atom type is described by individual partial pair distribution functions. Related feff files containing amplitude and phase information have to be generated for all absorber sites i and listed in rmc.the.i files contributing to spectrum I . Sites are identified by the 'atom type number' in rmc.ucc, rie.par or rmc.coo files depending on whether coordinates are generated by gencoo or input by incoo subroutines. The rmc.the.i files relate atom type numbers to elements through the feff-files (feffijkl.dat) and have to be consistent with rmc.ucc, rie.par or rmc.coo.

```
title zro2, monoclinic , NDP,RT, Howard et al. Acta Crys B44 (1988), 116
rmax=10.0   Space P 21/C
a=5.1505 b=5.2116 c=5.3173 alpha=90.0 beta=99.23 gamma=90   core = Zr1
atom
! At.type  x          y          z
  Zr       0.2754      0.0395      0.2083      Zr1
  O        0.0700      0.3317      0.3447      O1
  O        0.4496      0.7569      0.4792      O2
```

Fig. 5: Typical atoms.inp file

```

* This feff.inp file generated by ATOMS, version 2.42e
* ATOMS written by Bruce Ravel and copyright of The Univ. of Washington, 1994

* -- * -- * -- * -- * -- * -- * -- * -- * -- * -- * -- * -- * -- * -- *
*      total mu =      398.3 cm^-1, delta mu =      332.8 cm^-1
*      specific gravity = 5.809, cluster contains 361 atoms.
* -- * -- * -- * -- * -- * -- * -- * -- * -- * -- * -- * -- * -- * -- *
*      mcmaster corrections: 0.00025 ang^2 and 0.127E-06 ang^4
* -- * -- * -- * -- * -- * -- * -- * -- * -- * -- * -- * -- * -- * -- *

TITLE   zro2  monoclinic   NDP RT   Howard et al. Acta Crys B44

HOLE 1   1.0      1=k edge, s0^2=1.0

*      mphase,mpath,mfeff,mchi
CONTROL  1      1      1      1
PRINT    0      0      0      3

RMAX      9.9932

*CRITERIA      curved      plane
*DEBYE          temp      debye-temp
NLEG           2
*RMULTIPLIER   1.0

POTENTIALS
*   ipot   z   label
      0    40   Zr
      1     8    0
      2    40   Zr

ATOMS
  0.0000    0.0000    0.0000    0   Zr          0.0000
 -1.0442    1.5228    0.8950    1   01          2.0519
 -1.7559   -1.0830    0.0035    1   01          2.0631
  0.8856   -1.4728    1.2965    1   02          2.1528
 -1.0442    0.6713   -1.7637    1   01          2.1567
  1.3980    1.1330   -1.2242    1   02          2.1764
  0.8856   -1.5447   -1.3621    1   02          2.2418
  1.3980    1.0611    1.4345    1   02          2.2667
 -2.8002   -0.4117   -1.7602    2   Zr1         3.3330
  0.0000    2.1941    2.6586    2   Zr1         3.4471
  0.0000    2.1941   -2.6586    2   Zr1         3.4471
  2.2836    2.6058    0.0724    2   Zr1         3.4656
  2.2836   -2.6058    0.0724    2   Zr1         3.4656
  2.2836   -0.4117   -2.5863    2   Zr1         3.4747
  2.2836   -0.4117    2.7310    2   Zr1         3.5837
.
.
.
END

```

Fig. 6: Typical feff.inp file (modified output of atoms) to generate feffi.jkl.dat for single scattering paths. The red lines are different from standard feff.inp.

3.2 Procedure (flow of RMC analysis process)

The flow of a typical RMC analysis may be performed in four steps:

1. `rmcxas` runs on unix platforms (linux or Mac) as noninteractive program. It is recommended to place the `rmcxas` file in your 'bin' folder (e.g. `/usr/local/bin`)
2. Place all files for analysis in a single folder (one folder for each refinement is recommended).
3. Run the program `rmcxas` in the background using the unix command:

```
nohup rmcxas > rmcscreen &
```

this starts the refinement and generates a file `rmcscreen` (or any other name you choose) which contains some information about the status of `rmcxas` and all other output files depending on the modes of computation selected in `rmc.par`. The complete information about status and performance of `rmcxas` can be found in `rmc.log` (logging information input to or output by `rmcxas`) and `rmc.cyc` (logging information about performance of `rmcxas`).

4. Analyze output.

3.3 Limits of the code and hints for using it

- Limits due to physical size of arrays at present (can be modified on request), maximum number of
 - phases: `mphas = 3`
 - EXAFS spectra: `mspec = 3`
 - data in EXAFS spectra: `mdat = 1,024`
 - atoms in configuration: `matom = 100,000`
 - different atom types: `mtyp = 5`
 - bins in histogram of pPDFs: `mhis = 5,000`
 - diffractograms: `mdiff = 3`
 - data in diffractograms: `mdatd = 2048`
 - atoms in unit cell: `mu = 100`
 - parameters in Rietveld refinement: `mparr = 600`

- Periodic boundary conditions

The code uses implicitly periodic boundary conditions. Therefore, the size of the supercell (simulation box) needs to be larger than two times the maximum distance for the pPDFs.

- Amorphous configuration

The most simple way to generate an amorphous configuration is to use a crystalline model of the same atom number density and use `rmcxas` to randomize it (applying reasonable hard sphere radii) by setting the value of the error variable (`errmod`) in `rmc.par` to 100.0.

- Non-periodic models

For non-periodic models (for example cluster models for nanoparticles) the size of the supercell (simulation box) needs to be larger than two times the maximum distance for the pPDFs and two times the sum of the cluster radius plus the difference between simulation box edge length and cluster diameter.

- A typical sequence for Rietveld refinement of nanocrystalline materials is
 - 0 obtain reasonable initial parameters by manual adjustment and simulation
 - 1 refine scale and background offset (check background position parameter (# 20))

- 2 refine 1 + remaining background and shape parameters (u, x, y, d, ε)
- 3 refine 2 + lattice parameters and 2θ offset
- 4 refine 3 + mean square displacements
- 5 refine 4 + fractional coordinates

This type of sequential refinements can be performed by copying the `rie.fit` result to the `rie.par` file and resetting the parameter `atmov` to 1.0 before starting the next refinement step.

- confinement limits in `rie.par`, `axs.par` and `deb.par`

Confinement limits in `rie.par`, `axs.par` and `deb.par` should be used with care. In case the refinement runs into a parameter limit, one should adjust the limit generously, although physically realistic.

- simultaneous refinement of several data sets, especially EXAFS and scattering

Since the number of data and their signal amplitude of different data sets can be quite different, especially between EXAFS and scattering data, the ‘temperature’ parameters (line 28 and 31 in `rmc.par`) need to be adjusted to obtain χ^2 values of similar levels for the different data sets (these values are computed also during simulations without refinement and output in `rmc.log`).

- simultaneous analysis of XAFS by RMC and XRD by Rietveld

Depending on the coupling level, coupled parameters need to be variable in `rie.par`.

3.4 File type when using `rmcxas`

All control, input and output files are of type text (ASCII).

3.5 Control files (*.par)

- `rmc.par`

Main control file (compare Fig. 3 and 7).

Line Comment / Explanation

1	is a comment (up to 80 characters)
2	the first number is the number of phases <code>nphas</code> , followed by <code>nphas</code> pairs of numbers of number of scatterers <code>nscat</code> and absorbers <code>nabs</code> in each phase, the number of scatterers is the total number of different atom types in each phase, the number of absorbers in each phase can therefore not be larger
3	the first number is the number of spectra, the following numbers (as many as the total number of scatterers) assigns the atom types as absorbers to a spectrum (1 if for the first spectrum, also the first data file at line 28) and if the atom type is only a scatterer it is labeled by a 0 here.
4	number of scattering / diffraction data sets, identifier of scattering type for each data set (<code>x, n, or e</code>), computational mode for scattering / diffraction (<code>s, i, d, r</code>) and coupling level for Rietveld computational mode (0, 1, 2, 3)
5	input mode (<code>g, i, r, p</code>)
6	lattice constant a for each phase (in Å)
7	lattice constant b for each phase (in Å)
8	lattice constant c for each phase (in Å)
9	number of unit cells in a direction to generate supercell (simulation box)
10	number of unit cells in b direction to generate supercell (simulation box)
11	number of unit cells in c direction to generate supercell (simulation box)
12	lattice constants α for each phase (in degrees)

- 13 lattice constants β for each phase (in degrees)
- 14 lattice constants γ for each phase (in degrees)
- 15 fraction of phases
- 16 total number of different atom types (equal to `nscat` in line 2)
- 17 bin width for radial distribution
- 18 maximum radius for PDFs (EXAFS) and (Debye)
- 19 hard sphere radii (distances) for each partial pair distribution function
((`nscat*nscat+nscat`)/2)
- 20 maximum movement per MC step for each phase (in Å)
- 21 logical switch for coordination number constraints (if `.true.` `rmc.con` is needed).
- 22 number of RMC cycles (in each cycle each atom in the configuration with movement flag
of 1 is attempted to move once which is called a RMC step) (0 for simulation only)
- 23 number of cycles after which coordinates and refinement data are saved
- 24 weighting power for each EXAFS spectrum
- 25 E_0 shifts for each EXAFS spectrum (in eV)
- 26 amplitude reduction for each EXAFS spectrum
- 27 Debye-Waller factor (σ^2 in Å²) for each EXAFS spectrum (if < 0 applied in PDF, if > 0 :
applied in feff, if 0 not used)
- 28 error estimate for each EXAFS spectrum (if < 0 from data column, if > 0 : value is used,
if = 0 it is set to 1.0) (corresponds to the temperature in Metropolis type MC)
- 29 number of header lines, column number for independent (k), dependent (χ) and error (σ)
variable in EXAFS data set, file name of EXAFS data set (up to 31 characters); this line
has to be repeated for each EXAFS spectrum. No additional character is allowed behind
the filename. This line is repeated for each `nspec` filenames (sequence consistent with
`rmc.the.i`).
- 30 wavelength or acceleration voltage for each scattering data set (if negative a_1 and a_2
wavelength are used from a table for e-diffraction the acceleration voltage is used)
- 31 error estimate for each scattering data set (if < 0 `sqrt(y)` is used, if > 0 : value used, if =
0 it is set to 1.0, and if = 1 value from data column) (corresponds to the temperature in
Metropolis type MC)
- 32 number of header lines, columns number for independent (q), dependent (S or I) and error
(s) variable in scattering data set, file name of scattering data set (up to 31 characters);
this line has to be repeated for each scattering data set. No additional character is allowed
behind the filename. This line is repeated for each `ndiff` filenames (sequence consistent
with `rmc.aff`).

1	m-ZrO2	
2	1 2 1	nphas (<= 2), nscatt in phase 1, nabs in phase 1, 2, ...
3	1 1 0	nspec (number of spectra <= 3), listsit (absorber to spectrum)
4	2 x n r 2	ndiff (<=3), diffprobe (x,e,n), compmode ((d)ebye, (s)trf.)
5	g	imode (input mode for coord.(g)enerate,(i)nput,input&(r)estart)
6	5.151 3.9824	alatt (lattice parameter in x) for phase 1, 2, ...
7	5.207 3.9824	blatt (lattice parameter in y) for phase 1, 2, ...
8	5.319 6.2719	clatt (lattice parameter in z) for phase 1, 2, ...
9	4 16	hn (number of unit cells in x) for phase 1, 2, ...
10	4 16	kn (number of unit cells in y) for phase 1, 2, ...
11	4 10	ln (number of unit cells in z) for phase 1, 2, ...
12	90.0,90.0	alpha (in degrees) for phase 1, 2, ...
13	99.23,90.0	beta (in degrees) for phase 1, 2, ...
14	90.0,120.0	gamma (in degrees) for phase 1, 2, ...
15	1.0,0.0	fraction of phases for 1, 2 (normalized by program)
16	2	ntyp (total number of different atom types / scatterers / sites)
17	0.025	deltar (bin width for radial distributions)
18	10.0,10.0	rmax (maximum radius for radial distribution)
19	3.2 1.8 2.3	1.0 1.0 1.0 1.0 1.0 1.0 1.0 1.0 close(i),i=1,(ntyp*ntyp+ntyp)/2
20	0.05,0.025	drmax (maximum movement by Monte Carlo) for phase 1, 2
21	.false.	switch for coordination number constraints (from "rmc.con")
22	200	ncyc (number of cycles to perform)
23	1	nout (number of cycles after which coordinates etc. are saved)
24	3	power (power of k-vector)
25	-5.0 0.0	e0shift(j),j=1,nspec (e0-shift for feff, in eV)
26	1.0 1.0	s02(j),j=1,nspec (amplitude reduction factor for feff)
27	0.000 0.000	sig2(j),j=1,nspec (negative:in pdf,positive:in feff,0.0:none)
28	0.003 0.003	errmod(j),j=1,nspec (0.0: err(i)=1)
29	23,1,2,5,mw_0037to39.mcm	
30	-1.54 1.117 200000	wavelength (A) or acceleration voltage (V)
31	-1.0 0.05 100	errmod(j), j=1,nscatt (0.0: err(i)=1)
32	1,1,2,3,mzro2.xrd.dat	
33	0,1,2,3,mzro2.ndp.dat	

Fig. 7: Typical main control file rmc.par (blue are rmcxas control parameters, black text is commenting the lines, it is not read by rmcxas and can be changed individually). Lines 24 to 29 are not used when nspec = 0 (no EXAFS spectrum).

Additional explanations to lines 3 to 5:

- scattering type (choose up to 3)
 - x: X-rays as probe particles
 - n: neutrons as probe particles
 - e: electrons as probe particles
- computational mode for scattering / diffraction (choose one)
 - s: structure factor as dependent variable
 - i: scattering intensity as dependent variable computed via structure factor
 - d: scattering intensity as dependent variable computed via Debye scattering equation
 - r: diffraction intensity as independent variable computed via a Rietveld type approach
- coupling mode for Rietveld computational mode to EXAFS RMC (choose one)
 - 0: coupled only for generating initial atomic configuration (unit cell content)

- 1: Rietveld results transferred to EXAFS RMC
- 2: coupling mode 1 and EXAFS RMC results transferred to Rietveld
- 3: coupling mode 2 and transfer of Debye-Waller factors from Rietveld to EXAFS RMC
- input mode
 - g: generate atomic configuration from unit cell content in `rmc.ucc.i` for each phase *i*. This is automatically done when EXAFS RMC is coupled to Rietveld refinement information, however, the unit cell content is then taken from `rie.par` and optimized parameters.
 - i: atomic configuration is input from `rmc.coo.i` when `rmcxas` is started, the input coordinates are saved in `rmc.coo.ini.i` (replacing any existing file).
 - r: atomic configuration is input from `rmc.coo.i` when `rmcxas` is started, the input coordinates are saved in `rmc.coo.ini.i` (replacing existing file), the root mean square displacements of each atom is reset to 0.
 - p: production mode for statistical evaluation of simulation/refinement results: generates $j = 1, \dots, \text{ncyc}$ number of `rmc.coo.i.pj`, `rmc.spe.i.pj` and `rmc.pdf.i.pj` files (typically performed after convergence for `ncyc = 100`)
 - The input coordinates are saved in `rmc.coo.ini.i`.

`rmc.par` generates error codes when the input format is incorrect or information is missing by listing the corresponding line number of `rmc.par` in `rmc.log`.

- `axs.par`

Control file for refining low frequency background (LFS) in EXAFS data. In Fig. 8, the first 6 lines (blue) are control parameters for the MC code used to minimize χ^2 . `ngmcy` is the number of MC cycles for refining LFS, `ncycs` is the number of `rmc` cycles at which LSF refinement is starting and `ncyce` at which MC cycles are ending. `gnadjst` is the number of MC cycles after which the step size is adjusted, `gacrtio` is the corresponding acceptance ratio, `gadjst` the adjustment factor and `atmov` the multiplication factor for the step size which is adjusted.

The line starting with # is a header line describing the meaning of 9 columns of the following Rietveld parameters, the first column (#) is the parameter index used for parameter correlation. The second is the initial parameter value, the third the minimum parameter value, fourth the maximum parameter value, the fifth the step interval of the parameter (parameters are fixed/not refined if they are set to 0.0, typically it should be set to about 0.1% of the parameter value), the sixth is the index number of the parameter to which the parameter is correlated to (0 if no correlation), the seventh and eighth are the linear correlations coefficients *a* and *b* ($y = a \cdot x + b$, where *y* is the actual parameter correlated to the parameter *x*) and the last column is the parameter name (may be freely chosen, up to 20 characters without space). There are 6 parameters for each spectrum. If `ncycs` (in `axs.par`) > `ncyc` in (in `rmc.par`), the low frequency background is not refined.

```

1000 ngmcy: number of MC cycles for atomic xafs
1000,2000 ncycs,ncyce: # of rmc cycle at which MC cycles for axafs start & end
100 gnadjst: # of MC cycle after which step is adjusted
0.01 gacrtio acceptance ratio
0.01 gadjst adjustment factor
1.0 atmov
# para pmin pmax pmov 6 lines (parameters) per spectrum fitted in rmc
1 0.001,-1.0,1.0,0.001,0,0.0,0.0 a0      amp=a0*exp(-2.0*b1*a1)
2 0.1,0.001,1.0,0.001,0,0.0,0.0 a1      *exp(-2.0*a2*a2*k*k)/(b1*b1)
3 0.1,0.001,1.0,0.001,0,0.0,0.0 a2      pha=b0+2.0*b1*k+b2*k*k
4 -10.0,-20.0,20.0,0.1,0,0.0,0.0 b0      ysim=amp*sin(pha)*k**n
5 1.0,0.01,2.0,0.01,0,0.0,0.0 b1
6 0.1,-1.0,1.0,0.001,0,0.0,0.0 b2
7 0.001,-1.0,1.0,0.001,0,0.0,0.0 a0      amp=a0*exp(-2.0*b1*a1)
8 0.1,0.001,1.0,0.001,0,0.0,0.0 a1      *exp(-2.0*a2*a2*k*k)/(b1*b1)
9 0.1,0.001,1.0,0.001,0,0.0,0.0 a2      pha=b0+2.0*b1*k+b2*k*k
10 -10.0,-20.0,20.0,0.1,0,0.0,0.0 b0     ysim=amp*sin(pha)*k**n
11 1.0,0.01,2.0,0.01,0,0.0,0.0 b1
12 0.1,-1.0,1.0,0.001,0,0.0,0.0 b2

```

Fig. 8: Typical control file `axs.par` for fitting the low frequency signal in EXAFS (black is comment, blue are MC control parameters, and red are LFS fitting parameters).

- `deb.par`

Control file for refining scale (amplitude) factor and background for Debye scattering, scattering intensity computed from $S(q)$ or structure factor $F(q)$. In Fig. 9, the first 6 lines (blue) are control parameters for the MC code used to minimize χ^2 . `ngmcy` is the number of MC cycles for refining the scattering background, `ncycs` is the number of rmc cycles at which scattering background refinement is starting and `ncyce` at which MC cycles are ending. `gnadjst` is the number of MC cycles after which the step size is adjusted, `gacrtio` is the corresponding acceptance ratio, `gadjst` the adjustment factor and `atmov` the multiplication factor for the step size which is adjusted.

The line starting with # is a header line describing the meaning of 9 columns of the following background parameters for the Debye scattering equation refinement, the first column (#) is the parameter index used for parameter correlation. The second is the initial parameter value, the third the minimum parameter value, the fourth the maximum parameter value, the fifth the step interval of the parameter (parameters are fixed/not refined if they are set to 0.0, typically it should be set to about 0.1% of the parameter value), the sixth is the index number of the parameter to which the parameter is correlated to (0 if no correlation), the seventh and eights are the linear correlations coefficients ($y = a*x + b$, where y is the actual parameter correlated to the parameter x) and the last column is the parameter name (may be freely chosen, up to 20 characters). There are 8 parameters (red) for each scattering data set (repeated for each additional scattering data set). If `ncycs` (in `deb.par`) > `ncyc` in (in `rmc.par`), the scattering background is not refined. The first of eight parameters (`b0`) is the scale factor of the simulated data, in case of the structure factor $F(q)$ it may be computed using eq. 17.

```

1000 ngmcyc: number of MC cycles for atomic xafs
1,2000 ncycs,ncyce: # of rmc cycle at which MC cycles for axafs start & end
100 gnadjst: # of MC cycle after which step is adjusted
0.01 gacrteo acceptance ratio
0.01 gadjst adjustment factor
1.0 atmov
# para pmin pmax pmov 8 lines (parameters) per diffractogram fitted in rmc
1 0.391292 ,0.0001,1e6,0.00, 0,0.0,0.0 b0 ysim(i)=b0*bsim(i)+bck
2 0.0, -1000.,1000.,0.00, 0,0.0,0.0 b1 bck=b1+b2*(qv**2)/1.0+b3*1.0/(qv**2)+
3 0.0,-1.0,1.0,0.00,0,0.0,0.0 b2 b4*(qv**4)/2.0+b5*2.0/(qv**4)+
4 0.0,-1.0,1.0,0.00,0,0.0,0.0 b3 b6*(qv**6)/6.0+b7*6.0/(qv**6)
5 0.0,-1.0,1.0,0.00,0,0.0,0.0 b4 see Larson and Dreele GSAS 2004, p.132
6 0.0,-1.0,1.0,0.00,0,0.0,0.0 b5
7 0.0,-1.0,1.0,0.00,0,0.0,0.0 b6
8 0.0,-1.0,1.0,0.00,0,0.0,0.0 b7
9 5e7 ,0.0001,0.01,1.,0,0.0,0.0 b0 ysim(i)=b0*bsim(i)+bck
10 1000.0,-1000.,5000.,1.0,0,0.0,0.0 b1 bck=b1+b2*(qv**2)/1.0+b3*1.0/(qv**2)+
11 5000.0,-1.0,10000.0,0.001,0,0.0,0.0 b2 b4*(qv**4)/2.0+b5*2.0/(qv**4)+
12 0.0,-1.0,1.0,0.00,0,0.0,0.0 b3 b6*(qv**6)/6.0+b7*6.0/(qv**6)
13 0.0,-1.0,1.0,0.00,0,0.0,0.0 b4 see Larson and Dreele GSAS 2004, p.132
14 0.0,-1.0,1.0,0.00,0,0.0,0.0 b5
15 0.0,-1.0,1.0,0.00,0,0.0,0.0 b6
16 0.0,-1.0,1.0,0.00,0,0.0,0.0 b7
17 5e7 ,0.0001,0.01,1.,0,0.0,0.0 b0 ysim(i)=b0*bsim(i)+bck
18 5000.0,-1000.,50000.,1.0,0,0.0,0.0 b1 bck=b1+b2*(qv**2)/1.0+b3*1.0/(qv**2)+
19 0.0,-1.0,1.0,0.00,0,0.0,0.0 b2 b4*(qv**4)/2.0+b5*2.0/(qv**4)+
20 50000.0,-1.0,10000.0,1.00,0,0.0,0.0 b3 b6*(qv**6)/6.0+b7*6.0/(qv**6)
21 0.0,-1.0,1.0,0.00,0,0.0,0.0 b4 see Larson and Dreele GSAS 2004, p.132
22 0.0,-1.0,10000.0,.0,0,0.0,0.0 b5
23 0.0,-1.0,1.0,0.00,0,0.0,0.0 b6
24 0.0,-1.0,10000.0,.0,0,0.0,0.0 b7

```

Fig. 9: Typical control file `deb.par` for fitting the intensity and background variables in Debye scattering equation for up to 3 scattering data sets. (black is comment, blue are MC control parameters, and red are background fitting parameters)

- `rie.par`

Rietveld control file (only needed when Rietveld type refinement is selected). In Fig. 10, the first 6 line (blue) are control parameters for the MC code used to minimize χ^2 . `ngmcyc` is the number of MC cycles for Rietveld refinement (recommended 1000), `ncycs` is the number of rmc cycles at which the Rietveld refinement is starting, `ncyce` at which MC cycles are ending and `ncycex` after how many rmc cycles the Rietveld refinement is repeated. `gnadjst` is the number of MC cycles after which the step size is adjusted (recommended 100), `gacrteo` is the corresponding acceptance ratio, `gadjst` the adjustment factor and `atmov` the multiplication factor for the step size which is adjusted (recommended 1 to 10). Changing `atmov` is a method to modify the step size for all parameters according to this factor.

The line starting with `#` is a header line describing the meaning of 9 columns of the following Rietveld parameters, the first column (`#`) is the parameter index used for parameter correlation. The second is the initial parameter value, the third the minimum parameter value, the fourth the maximum parameter value, the fifth the step interval of the parameter (parameters are fixed/not refined if the step intervals are set to 0.0, typically it should be set to about 0.1% of the

```

1000 ngmcyc
1,10, 10 ncyce, ncyce, ncyce
10 nadjst
0.01 acrtio
0.01 adjst
1.0 atmov
# fitting parameter, min, max, mov, icrr, acrr, bcrr, name
1 1.900000E+01 1.000000E-02 100.0000 1.000000E+00 0 0.0 0.0 intensity_scale
2 1.000000E-03 1.000000E-04 0.10000 0.000000E-05 0 0.0 0.0 offset 2theta
3 1.000000E-03 1.000000E-04 0.10000 0.000000E-05 0 0.0 0.0 sample displ.
4 1.000000E-03 1.000000E-04 0.10000 0.000000E-05 0 0.0 0.0 transparency
5 0.0078300 0.000000 0.100000 0.000000E-04 0 0.0 0.0 u_cagliotti
6 -0.0078800 -0.100000 0.100000 0.000000E-04 0 0.0 0.0 v_cagliotti
7 0.0094300 -0.100000 0.100000 0.000000E-04 0 0.0 0.0 w_cagliotti
8 50.0000 1.000000E-04 300.000 0.1000 0 0.0 0.0 backgr0
9 -90.000 -2.000000E+02 200.000 0.10000 0 0.0 0.0 backgr1
10 0.000 -1.000000E+02 120.000 0.01000 0 0.0 0.0 backgr2
11 0.000000 1.000000E-02 120.000 0.000000 0 0.0 0.0 backgr3
12 0.000000 1.000000E-02 120.000 0.000000 0 0.0 0.0 backgr4
13 0.000000 1.000000E-02 120.000 0.000000 0 0.0 0.0 backgr5
14 0.000000 1.000000E-02 120.000 0.000000 0 0.0 0.0 backgr6
15 0.000000 1.000000E-02 120.000 0.000000 0 0.0 0.0 backgr7
16 0.000000 1.000000E-02 120.000 0.000000 0 0.0 0.0 backgr8
17 0.000000 1.000000E-02 120.000 0.000000 0 0.0 0.0 backgr9
18 0.000000 1.000000E-02 120.000 0.000000 0 0.0 0.0 backgr10
19 0.000000 1.000000E-02 120.000 0.000000 0 0.0 0.0 backgr11
20 30.00000 1.000000E-02 120.000 0.000000 0 0.0 0.0 backgrposition
21 0.950000 1.000000E-04 1.00000 0.010000 0 0.0 0.0 phasefraction
22 40. 1.00000 100000.0 0.100000 0 0.0 0.0 columnlength(A)
23 1.000000E-02 0.000001 1.000000E-02 1.000000E-04 0 0.0 0.0 microstrain
24 3.632000 1.00000 10.0000 1.000000E-04 0 0.0 0.0 alatt(A)
25 3.632000 1.00000 10.0000 0.000000E-04 24 1.0 0.0 blatt(A)
26 5.186000 1.00000 10.0000 1.000000E-06 0 0.0 0.0 clatt(A)
27 90.00000 0.000000 0.000000 0.000000 0 0.0 0.0 alphad(deg)
28 90.00000 90.0000 120.000 0.000000E-03 0 0.0 0.0 betad(deg)
29 90.0000 0.000000 0.000000 0.000000 0 0.0 0.0 gammd(deg)
30 7.0000 0.000000 0.000000 0.000000 0 0.0 0.0 nsit1
31 1.00000 0.000000 0.000000 0.000000 0 0.0 0.0 atomtype1
32 0.90000 0.000000 1.000000 0.01 0 0.0 0.0 occ1
33 0.750000 0.000000 1.00000 0.00000 0 0.0 0.0 xuc1
34 0.250000 0.000000 1.00000 0.00000 0 0.0 0.0 yuc1
35 0.750000 0.000000 1.00000 0.00000 0 0.0 0.0 zuc1
36 8.000000E-03 0.000000 0.100000 0.0001 0 0.0 0.0 umsq1
.
.
.

```

Fig. 10: Structure of the `rie.par` file. Blue: MC control parameters, red: instrumental parameters (repeated for each diffractogram), green microstructural and crystallographics parameters and orange: unit cell parameters (green and orange are repeated for each crystallographic phase, orange for each site in the unit cell).

parameter value), the sixth is the index number of the parameter to which the parameter is correlated to (0 if no correlation), the seventh and eights are the linear correlations coefficients ($y = a*x + b$, where y is the actual parameter correlated to the parameter x) and the last column is the parameter name (may be freely chosen, up to 20 characters).

The first 20 parameters (red) are instrumental parameters for each diffractogram (repeated for each additional diffractogram), the next 9 parameters (green) are the microstructural and crystallographic parameters for each phase and the remaining parameters (orange) describe the contents of the unit cell ($n_{\text{sit}} \times 6$) the first the atom type (not refinable, is converted to integer in the code and should be consistent with EXAFS), occupancy, fractional coordinates x , y , z and mean square displacement (Debye-Waller-factor). If site-parameters have identical fractional coordinates, this is interpreted as substitution (the occupation parameters add up to 1). The ‘green’ and ‘orange’ parameters are repeated for each phase.

The variable parameters are attempted to change in every MC cycle once according to the step size indicated, correlated parameters are computed according to the linear correlation rule in `rie.par`. The step size by which the variable parameters are changed is provided in `rie.par` but may be adjusted to improve the acceptance ratio. If the MC guess of a parameter falls outside the confinement interval in `rie.par` it is discarded (not accepted). For each MC step the first and second moment of all variable parameters weighted by χ^2 are computed. These values are used after the final MC cycle to compute the variance (standard deviation) of the parameters. The final result is corresponding to the minimum χ^2 (joined for all diffractograms analyzed simultaneously). Problems may arise if the step size is wrongly chosen. If a parameter is not sampled, for example due to an inappropriate confinement interval or step size, the error estimate will be showing a value of zero. The variable parameters may not have been changed during the MC refinement either because the initial value is outside the confinement interval or the step size is too large or since the number of cycles is too small. This may be indicated by a value of 0.0 for the error estimates in the `rie.res` file. The correlation of the site parameters may be used to enforce the missing point symmetry to the P1 Rietveld refinement. If `ncycs` (in `deb.par`) > `ncyc` in (in `rmc.par`), Rietveld refinement is not performed.

- `rmc.con`

File containing constraints, only used when logical switch in `rmc.par` is ‘.true.’ with as many lines as constraints. These constraints might be helpful for molecular type systems. The meaning of the columns is

- 1 number of pPDF (integer)
- 2 starting radial distance over which to compute the coordination number (real)
- 3 ending radial distance over which to compute the coordination number (real)
- 4 target value for coordination number (real)
- 5 ‘temperature’ (weight) of constraint (real)

3,1.6,2.3,0.66,0.01 pdf number,r1,r2,CNtarget,sigma
--

Fig. 11: Structure of the `rmc.con` file.

3.6 Input files

- `rmc.ucc.i`

File containing information about atoms in the unit cell. This file is used if the input mode is `g` in `rmc.par`. The `p1.inp` file generated by `atoms` can be used after editing. The meaning of the columns is

- 1 index (integer)
- 2 fractional coordinate x (real)
- 3 fractional coordinate y (real)

- 4 fractional coordinate z (real)
- 5 occupation number o (optional) (real), if missing, it is set to 1.0.

```

1 0.275235 3.848076E-02 0.209347
2 7.002163E-02 0.332314 0.336058
2 0.449459 0.758194 0.477776
1 0.726547 0.540409 0.292504
2 0.929836 0.832161 0.165522
2 0.550097 0.258802 2.379632E-02
1 0.724354 0.958649 0.790371
2 0.928158 0.668465 0.663994
2 0.550655 0.244912 0.522966
1 0.274534 0.459190 0.710121
2 7.017633E-02 0.167950 0.835865
2 0.449755 0.741009 0.979191

```

Fig. 12: Structure of the `rmc.ucc.i` file. (from `p1.inp` output by atoms) (12 lines for each site in unit cell (P1))

- `rmc.coo.ini.i`, `rmc.coo.i`

File containing information about the atoms in the simulation box. The meaning of the columns is

- 1 index (integer)
- 2 atom type (integer)
- 2 cartesian coordinate x (Å) (real)
- 3 cartesian coordinate y (Å) (real)
- 4 cartesian coordinate z (Å) (real)
- 5 accumulated root mean square displacement
- 6 movement tag (0 if atom should not be moved by MC, 1 if it should be moved) (real)

```

1 1 -7.18521 -10.2686 -9.40208 0.248472 1.00000
2 2 -8.49194 -9.03347 -8.62588 26.1191 1.00000
3 2 -7.11041 -6.28602 -7.96792 22.3067 1.00000
4 1 -5.17463 -7.66150 -9.06069 0.137668 1.00000
5 2 -3.99506 -5.88812 -9.39131 18.2340 1.00000
6 2 -5.68679 -9.07913 -10.4146 21.2810 1.00000
7 1 -5.63195 -5.49743 -6.40785 0.223186 1.00000
8 2 -5.04399 -7.46799 -6.86633 17.5452 1.00000
.
.
.

```

Fig. 13: Structure of the `rmc.coo.i` file.

- `rmc.the.i`

List of feff scattering paths `ijhk` information contained in `feffi.jhk.dat` files for each type of absorber atom *i* sorted by type of scattering atom *l*. The meaning of the columns is

- 1 atom type *l* (integer)
- 2 path to feff file `feffi.jhk.dat` (character)

```
1  ./feff/feff0008.dat
.
.
.
1  ./feff/feff0123.dat
2  ./feff/feff0001.dat
.
.
.
2  ./feff/feff0090.dat
```

Fig. 14: Structure of the `rmc.the.i` file pointing to the `feffi.jkl.dat` files in folder/directory ‘feff’

- `feffijkl.dat`

Files generated by feff containing EXAFS kernel information for all (single scattering) paths.

```
zro2 monoclinic NDP RT Howard et al. Acta Crys B44 Feff 8.10
Abs Z=40 Rmt= 1.436 Rnm= 1.527 K shell
Pot 1 Z= 8 Rmt= 0.992 Rnm= 1.083
Pot 2 Z=40 Rmt= 1.440 Rnm= 1.535
Gam_ch=4.800E+00 H-L exch
Mu= 8.781E-01 kf=2.263E+00 Vint=-1.863E+01 Rs_int= 1.603
Path 1 icalc 2
-----
2 1.000 2.0519 2.4007 0.87810 nleg, deg, reff, rnrnav(bohr), edge
    x y z pot at#
    0.0000 0.0000 0.0000 0 40 Zr absorbing atom
-1.0442 1.5228 0.8950 1 8 0
k real[2*phc] mag[feff] phase[feff] red factor lambda real[p]@#
0.000 8.1478E+00 0.0000E+00 -8.9614E+00 1.112E+00 7.1972E+00 2.2669E+00
0.100 8.1462E+00 4.6055E-02 -9.3645E+00 1.112E+00 7.2039E+00 2.2690E+00
0.200 8.1414E+00 9.1671E-02 -9.7532E+00 1.111E+00 7.2237E+00 2.2753E+00
.
.
.
```

Fig. 15: Structure of `feffijkl.dat` files here the `feff0001.dat` for m-ZrO₂

- `rmc.aff.i`

File containing 9 Cromer-Mann type coefficients (for example from Maslen et al. 2006) to compute atom form factors for every scattering / diffraction for data set *i*. Each line in

18.1668	1.21480	10.0562	10.1483	1.01118	21.6054	-2.64790	-0.102760	9.41454
3.75040	16.5151	2.84294	6.59203	1.54298	0.319201	1.62091	43.348600	0.24206

- 'exafs.dat'

```
# 22:31:43 11/ 4/ 1 mw_0037to39.mcm
# Heraeus ZrO2 powder in apiezon RT
# xafs version: 2.6 u MW10/10/96
#
# input: hasa1; average absolute error:   0.118575
#
# preedge: mode: victor
# E0fit: E0=    18011.5      step=    1.24411      mode: el0
# E0fit: width=    8.50610
# avg: no. of averaged data sets:    3
# bkg: kpower 3.0 # of knots: 9 mode: spline+error
# ksmooth: interval of k-space grid: 0.4000E-01
# McMa: zrk 17.990/keV and ai    12.8          0.697        -0.789          0.565E-01
#
#
#
#
#
#
#
#
#
#
k*Å           chi(McMaster) chi            McMaster         error(absolut
0.606264      0.693617E-01  0.693485E-01  1.00019          0.512287E-03
0.793739      0.111084       0.111048      1.00033          0.156114E-02
0.944716      0.165793       0.165716      1.00046          0.219492E-02
.
.
.
```

27

- 'scatt.dat'

Any file name (maximum 31 characters long) as many as scattering / diffraction data sets (X-ray, neutron and electron diffraction): either structure factor or scattering intensity as a function of scattering vector q (\AA^{-1}). Column oriented free format including header. Number of header lines, and columns for S , I , q and an error estimate (optional) have to be indicated in `rmc.par`.

```
# q intensity error
1.41513      40.0000      6.32460
1.41863      46.0000      6.78230
1.42213      24.0000      4.89900
1.42563      35.0000      5.91610
1.42913      40.0000      6.32460
1.43263      48.0000      6.92820
.
.
.
```

Fig. 18: Structure of a typical 'scatt.dat' file.

3.7 Output files

Be aware: output files are replaced upon restarting rmcxas.

- `rmc.log`

Logging all input and output information including important results.

- `rmc.cyc`

Logging performance of `rmcxas`, especially R -values for all data sets refined as a function of RMC cycle.

column 1: number of RMC cycle (`icyc`)

column 2: acceptance ratio of RMC steps

column 3: ratio of RMC steps where moves are prohibited by hard sphere radii

column 4: fitting index R for 1st scattering / diffraction or EXAFS data set

column k : $k = 4, \dots, 4 + \text{ndiff} + \text{nexafs}$ fitting indices R (%)

column l : sum of all root mean square displacement in `icyc`

column m : center of gravity of atoms in supercell

- `rmc.coo.ini.i`, `rmc.coo.i`

Atom configuration (physical model) after RMC simulation using initial parameters and after RMC refinement.

column 1: number of atom (integer)

column 2: type of atom (integer)

column 3: cartesian x coordinate (real) (\AA)

column 4: cartesian y coordinate (real) (\AA)

column 5: cartesian z coordinate (real) (\AA)

column 6: root mean square displacement (real) (\AA)

column 7: movement tag (atom is attempted to move when value is 1.0, atom is fixed when value is 0.0)

- `rmc.ucc.fit.i`

Information about unit cell content after Rietveld refinement in '`rmc.ucc.i`' format for each phase *i*.

column 1: type of atom (integer)
column 2: fractional x coordinate (real)
column 3: fractional y coordinate (real)
column 4: fractional z coordinate (real)
column 5: fractional occupation number
column 6: mean square displacement (real)
column 7 (only in first row): microstrain (real)

- `rmc.spe.ini.i`, `rmc.spe.i`

EXAFS spectrum after RMC simulation using initial parameters for spectrum *i* and after RMC refinement.

column 1: wave vector k ($1/\text{\AA}$) (real)
column 2: exafs data weighted by k^n , n chosen in `rmc.par` (real)
column 3: total exafs computed weighted by k^n , n chosen in `rmc.par` (real)
column 4: exafs (no LSF) weighted by k^n , n chosen in `rmc.par` (real)
column 5: LSF (low frequency signal fitted) (real)
column 6: residual (column 2 - column 3) (real)
column 7: error (RMC 'temperature') (real)

- `rmc.pdf.ini`, `rmc.pdf`

Partial pair distribution function after RMC simulation using initial parameters and after RMC refinement.

column 1: radial distance (\AA) (real)
column 2n: $n = 1, (\text{ntyp} \times \text{ntyp} + \text{ntyp})/2$; g_{ij} (real)
column 2n+1: coordination number = $4 \times \pi \times \rho \times \text{integral}(g_{ij})$ (real)

- `axs.cyc`

Logging performance of `rmcxas` regarding the fitting the low frequency background signal in EXAFS as a function of MC cycles.

column 1: number of MC cycle (integer)
column 2: order number of LSF parameter (integer)
column 3: chi-square (real)
column 4: acceptance ratio (real)
column 5: multiplier in maximum change per MC step (adjusted depending on acceptance ratio) (real)
column 6: fitting index R (%) (real)

- `axs.fit`

Results of fitting the low frequency signal in EXAFS in `axs.par` format to enable successive refinements.

- `deb.cyc`

Logging performance of `rmcxas` regarding the fitting the background using the Debye scattering equation as a function of MC cycles.

column 1: number of MC cycle (integer)
column 2: order number of background parameter (integer)
column 3: chi-square (real)
column 4: acceptance ratio (real)
column 5: multiplier in maximum change per MC step (adjusted depending on

acceptance ratio) (real)
column 6: fitting index R (%) (real)

- `deb.fit`

Results of fitting the background using the Debye scattering equation in `deb.par` format to enable successive refinements.

- `rmc.rie.ini.i`, `rmc.rie.i`, (`rmc.sca.ini.i`, `rmc.sca.i`)

Diffractiongram after Rietveld (scattering) simulation using initial parameters for diffractiongram *i* and after Rietveld (scattering) refinement.

column 1: q ($1/\text{\AA}$) (real)
column 2: 2θ (degrees) (real)
column 3: experimental intensity (real)
column 4: computed intensity (real)
column 5: computed background (real)
column 6: residual (column 2 - column 3) (real)
column 7: error (MC 'temperature') (real)

- `latdis.dat.i.j`

Positions of Bragg reflections for phase *i* and diffractiongram *j*.

column 1: number of Bragg reflection (integer)
column 2: 2θ (degrees) (real)
column 3: q ($1/\text{\AA}$) (real)
column 4: d-value (real)
column 5: *h* (integer)
column 6: *k* (integer)
column 7: *l* (integer)
column 8: position (on intensity scale) for displaying columns 5 to 7 (real)

- `rie.cyc`

Logging performance of `rmcxas`, especially *R*-values for the Rietveld refinement of diffraction data as a function of MC cycles.

column 1: number of MC cycle (integer)
column 2: order number of Rietveld parameter (integer)
column 3: value of Rietveld parameter (real)
column 4: chi-square (real)
column 5: acceptance ratio (real)
column 6: multiplier in maximum change per MC step (adjusted depending on acceptance ratio) (real)
column 7-9: fitting indices of computed diffractiongrams (up to 3) *R* (%) (real)

- `rie.res`

Refined Rietveld parameters with error estimates and improved readability.

- `rie.fit`

Refined Rietveld parameters in the format of the `rie.par` input file to enable successive refinements.

4 References

- M. P. Allen and D. J. Tildesley, Oxford University Press, Oxford **1987**
- D. Balzar, N. Audebrand, M. R. Daymond, A. Fitch, A. Hewat, J. I. Langford, A. Le Bail, D. Louër, O. Masson, C. N. McCowan, N. C. Popa, P. W. Stephens and B. H. Toby, *Size-strain line-broadening analysis of the ceria round-robin sample*, J. Appl. Cryst. **37** (2004) 911-924
- D. L. Bish and S. A. Howard, *Quantitative Phase Analysis Using the Rietveld Method*, J. Appl. Cryst. **21** (1988) 86-91
- A. Bolzan, C. Fong, B. J. Kennedy and C. Howard, *Structural Studies of Rutile-Type Metal Dioxides*, Acta Cryst. **B53** (1997) 373-380
- N. E. Cusack, *The Physics of Structurally Disordered Matter*, IOP Publishing Ltd **1987**
- P. D'Angelo, A. Di Cicco, A. Filipponi, and N. V. Pavel, *Double-electron excitation channels at the Br-K edge of HBr and Br₂*, Phys. Rev. A **47** (1993) 2055-2063
- A. Filipponi, E. Bernieri, and S. Mobilio, *Multielectron excitations in x-ray-absorption spectra of a-Si:H*, Phys. Rev. B **38** (1988) 3298-3304
- A. Filipponi, *The radial distribution function probed by X-ray absorption spectroscopy*, J. Phys.: Condens. Matter **6** (1994) 8415 – 8427. doi.org/10.1088/0953-8984/6/41/006
- J. Geiss, T. Falk, S. Ognjanovic, S. Anke, B. Peng, M. Muhler, and M. Winterer, *Atom Pair Frequencies as a Quantitative Structure–Activity Relationship for Catalytic 2-Propanol Oxidation over Nanocrystalline Cobalt–Iron–Spinel*, J. Phys. Chem. C **126** (2022) 10346–10358
- S. J. Gurmman and R. L. McGreevy, *Reverse Monte Carlo simulation for the analysis of EXAFS data*, J. Phys. Cond. Matter **2** (1990) 9463-9473
- R. J. Hill, chapter 5, *Data collection strategies: fitting the experiment*, in R. A. Young, *The Rietveld Method*, Oxford University Press **1995**
- G. Hölzer, M. Fritsch, M. Deutsch, J. Härtwig, and E. Förster, *K_{a1,2} and K_{b1,3} X-ray emission lines of the 3d transition metals*, Phys. Rev. B **56** (1997) 4554-4568
- B. W. Holland, J. B. Pendry, R. F. Pettifer, and J. Bordas, *Atomic origin of structure in EXAFS experiments*, J. Phys. C: Solid State Phys. **11** (1978) 633-642
- A. C. Larson and R. B. Von Dreele, *General Structure Analysis System (GSAS)*, Los Alamos National Laboratory Report LAUR **86-748** (2004), 130
- P. A. Lee, B. K. Teo, and A. L. Simons, *EXAFS: a New Parameterization of Phase Shifts*, J. Am. Chem. Soc. **99** (1977) 3856-3859
- V. Mackert, T. Winter, S. Jackson, R. Kalia, A. Levish, S. Lukic, J. Geiss, and M. Winterer, *Very Small Nanocrystalline Tin Dioxide Particles: Local-, Crystal-, and Micro-Structure*, J. Phys. Chem. C **127** (2023) 17389–17405
- E. N. Maslen, A. G. Fox and M. A. O'Keefe, *Coefficients for analytical approximation to the scattering factors of Tables 6.1.1.1 and 6.1.1.3*, International Tables for Crystallography (2006). Vol. C. ch. 6.1, pp. 578-580, Table 6.1.1.4 (<https://onlinelibrary.wiley.com/iucr/itc/Cb/ch6o1v0001/table6o1o1o4/>)
- R. L. McGreevy and L. Pusztai, *Reverse Monte Carlo simulation: a new technique for the determination of disordered structures*, Mol. Simul. **1** (1988) 359-367
- V. K. Pecharsky and P. Y. Zavalij, *Fundamentals of Powder Diffraction and Structural Characterization of Materials*, 2nd edition Springer **2009**
- J. J. Rehr, J. J. Kas, F. D. Vila, M. P. Prange, and K. Jorissen, *Parameter-free calculations of x-ray spectra with FEFF9*, Phys. Chem. Chem. Phys. **12** (2010) 5503-5513.
- J. J. Rehr, C. H. Booth, F. Bridges, and S. I. Zabinsky, *X-ray-absorption fine structure in embedded atoms*, Phys. Rev. B **49** (1994) 12347-12350
- J. W. Richardson, chapter 6, *Background Modeling in Rietveld Analysis*, in R. A. Young, *The Rietveld Method*, Oxford University Press **1995**

- B. K. Teo, *EXAFS: Basic Principles and Data Analysis*, Springer-Verlag Berlin Heidelberg **1986**
- B. K. Teo, P. A. Lee, A. L. Simons, P. Eisenberger, and B. M. Kincaid, *EXAFS: Approximation, Parametrization, and Chemical Transferability of Amplitude Functions*, J. Am. Chem. Soc. **99** (1977) 3854-3856
- M. Winterer, *Nanocrystalline Ceramics – Synthesis and Structure*, Springer, Heidelberg **2002**, Springer Series in Materials Science, Volume 53, ISBN 3-540-43433-X
- M. Winterer, *Coupling Rietveld refinement of X-ray diffraction data and Reverse Monte Carlo analysis of Extended X-ray Absorption Fine Structure spectra*, accepted by J. Mater. Res. **2025**
- M. Winterer, M., *Reverse Monte Carlo Analysis of EXAFS Spectra of Amorphous and Monoclinic Zirconia*, J. Appl. Phys. **88** (2000), 5635-5644
- M. Winterer, B. Delaplane, R. McGreevy, *X-Ray Diffraction, Neutron Scattering and EXAFS Spectroscopy of Monoclinic Zirconia: Analysis by Rietveld Refinement and Reverse Monte Carlo Simulations*, J. Appl. Cryst. **35** (2002), 434-442
- M. Winterer and J. Geiß, *Combining reverse Monte Carlo analysis of X-ray scattering and extended X-ray absorption fine structure spectra of very small nanoparticles*, J. Appl. Cryst. **56** (2023) 103-109
- R. A. Young, chapter 1, *Introduction to the Rietveld Method*, in R. A. Young, *The Rietveld Method*, Oxford University Press **1995**

5 Publications related to rmexas

Books

M. Winterer, *Nanocrystalline Ceramics – Synthesis and Structure*, Springer, Heidelberg **2002**, Springer Series in Materials Science, Volume 53, ISBN 3-540-43433-X

Book Chapters

R. Djenadic and M. Winterer, *Chemical Vapor Synthesis of Nanocrystalline Oxides*, p. 49-76, chapter 2, in Axel Lorke, Markus Winterer, Roland Schmechel, und Christof Schulz (eds.), *Nanoparticles from the Gas Phase – Formation, Structure, Properties*, Springer Berlin **2012**

Peer Reviewed

M. Winterer, *Coupling Rietveld refinement of X-ray diffraction data and Reverse Monte Carlo analysis of Extended X-ray Absorption Fine Structure Spectra*, J. Mater. Res. (**2025**) 13pp.

V. Mackert, T. Winter, S. Jackson, R. Kalia, A. Levish, S. Lukic, J. Geiss, and M. Winterer, *Very Small Nanocrystalline Tin Dioxide Particles: Local-, Crystal-, and Micro-Structure*, J. Phys. Chem. C **127** (2023) 17389–17405

J. Geiss, J., Bueker, J., Schulte, J., Peng, B., Muhler, M., Winterer, M., *LaCo_{1-x}Fe_xO₃ Nanoparticles in Cyclohexene Oxidation*, J. Phys. Chem. C **127** (2023) 5029–5038

M. Winterer and J. Geiß, *Combining reverse Monte Carlo analysis of X-ray scattering and extended X-ray absorption fine structure spectra of very small nanoparticles*, J. Appl. Cryst. **56** (2023) pp. 7

J. Geiss, J. Schulte, and W. Winterer, *Flash evaporation of low volatility solid precursors by a scanning infrared laser*, J. Nanopart. Res. **24** (2022) 248, 10pp.

A. Levish and M. Winterer, *Formation of polymorphs and pores in small nanocrystalline iron oxide particles*, Sci. Rep. **12** (2022) 15291, 11pp

J. Geiss, T. Falk, S. Ognjanovic, S. Anke, B. Peng, M. Muhler, and M. Winterer, *Atom Pair Frequencies as a Quantitative Structure–Activity Relationship for Catalytic 2-Propanol Oxidation over Nanocrystalline Cobalt–Iron–Spinel*, J. Phys. Chem. C **126** (2022) 10346–10358

A. Levish and M. Winterer, *In situ cell for x-ray absorption spectroscopy of low volatility compound vapors*, Rev. Sci. Instr. **91** (2020) 063101, 7pp

S. M. Ognjanovic, M. Zähres, C. Mayer, and M. Winterer, *Local Structure of Nanocrystalline Aluminum Nitride*, J. Phys. Chem. C **122** (2018) 23749-23757

A. Kompch, A. Sahu, Chr. Notthoff, F. Ott, D. J. Norris, and M. Winterer, *Localization of Ag Dopant Atoms in CdSe Nanocrystals by Reverse Monte Carlo Analysis of EXAFS Spectra*, J. Phys. Chem. **119** (2015) 18762-18772

- A. Sandmann, A. Kompch, V. Mackert, Chr. Liebscher, M. Winterer, *Interaction of L-Cysteine with ZnO: Structure, Surface Chemistry, and Optical Properties*, *Langmuir* **31** (2015) 5701-5711
- R. Djenadic, G. Akgul, K. Attenkofer, and M. Winterer, *Chemical Vapor Synthesis and Structural Characterization of Nanocrystalline $Zn_{1-x}Co_xO$ ($x=0-0.50$) Particles by X-ray Diffraction and X-ray Absorption Spectroscopy*, *J. Phys. Chem.* **114** (2010) 9207-9215
- L. Schneider, S.V. Zaitsev, W. Jin, A. Kompch, M. Winterer, M. Acet, and G. Bacher, *Fabrication and analysis of Cr-doped ZnO nanoparticles from the gas phase*, *Nanotechnology* **20** (2009) 135604
- W. Jin, I. K. Lee, A. Kompch, U. Dörfler, and M. Winterer, *Chemical vapor synthesis and characterization of chromium doped zinc oxide nanoparticles*, *J. Eur. Ceram. Soc.* **27** (2007) 4333-4337
- J. U. Brehm, M. Winterer, and H. Hahn, *Synthesis and local structure of doped nanocrystalline zinc oxides*, *J. Appl. Phys.* **100** (2006) 064311
- Th. Enz, M. Winterer, B. Stahl, S. Bhattacharya, G. Miehe, K. Foster, C. Fasel, and H. Hahn, *Structure and Magnetic Properties of Iron Nanoparticles Stabilized in Carbon*, *J. Appl. Phys.* **99** (2006) 044306
- I. Berrodier, F. Farges, M. Benedetti, M. Winterer, G. E. Brown, M. Deveughele, *Adsorption mechanisms of trivalent gold on iron- and aluminum-(oxy)hydroxides. Part 1: X-ray absorption and Raman scattering spectroscopic studies of Au(III) adsorbed on ferrihydrite, goethite, and boehmite*, *Geochim. Cosmochim. Acta* **68** (2004) 3019
- M. Winterer, B. Delaplane, R. McGreevy, *X-Ray Diffraction, Neutron Scattering and EXAFS Spectroscopy of Monoclinic Zirconia: Analysis by Rietveld Refinement and Reverse Monte Carlo Simulations*, *J. Appl. Cryst.* **35** (2002) 434
- M. Winterer, *Reverse Monte Carlo Analysis of EXAFS Spectra of Amorphous and Monoclinic Zirconia*, *J. Appl. Phys.* **88** (2000) 5635

6 Appendices

6.1 Conversion between descriptors of phase composition

Molar fraction x_k of phase k (using mole numbers n_k):

$$x_k = \frac{n_k}{\sum_k n_k} \quad (\text{a1})$$

Number of atoms type l in phase k , γ_{lk} is the stoichiometric coefficient (N_A Avogadro constant):

$$N_{lk} = n_k \gamma_{lk} N_A \quad (\text{a2})$$

Atom fraction a_{lk} of atom type l in phase k :

$$a_{lk} = \frac{N_{lk}}{\sum_l N_{lk}} \quad (\text{a3})$$

Volume fraction v_k of phase k :

$$v_k = \frac{V_k}{\sum_k V_k} \quad (\text{a4})$$

Number densities ρ_k :

$$N_{lk} = \rho_k V_k a_{lk} = N_k a_{lk} \quad (\text{a5})$$

$$V_k = \frac{N_{lk}}{\rho_k a_{lk}} = \frac{n_k \gamma_{lk} N_A}{\rho_k a_{lk}} \quad (\text{a6})$$

$$v_k = \frac{\frac{n_k \gamma_{lk} N_A}{\rho_k a_{lk}}}{\sum_k \frac{n_k \gamma_{lk} N_A}{\rho_k a_{lk}}} = \frac{\frac{n_k}{\rho_k}}{\sum_k \frac{n_k}{\rho_k}}, \text{ since } \frac{\gamma_{lk} N_A}{a_{lk}} \text{ is constant for phase } k \quad (\text{a7})$$

$$n_k = x_k \sum_k n_k \quad (\text{a8})$$

$$v_k = \frac{\frac{x_k}{\rho_k} \sum_k n_k}{\sum_k \frac{x_k}{\rho_k} \sum_k n_k} = \frac{\frac{x_k}{\rho_k}}{\sum_k \frac{x_k}{\rho_k}} \quad (\text{a9})$$

$$a_{lk} = \frac{\gamma_{lk}}{\sum_l \gamma_{lk}} \quad (\text{a10})$$

$$\frac{\gamma_{lk}}{a_{lk}} = \sum_l \gamma_{lk} \quad (\text{a11})$$

From (a10) and (a1) follows:

$$n_k = \rho_k v_k \sum_k \frac{n_k}{\rho_k} \quad (\text{a12})$$

and

$$x_k = \frac{\rho_k v_k \sum_k \frac{n_k}{\rho_k}}{\sum_k \rho_k v_k \sum_k \frac{n_k}{\rho_k}} = \frac{\rho_k v_k}{\sum_k \rho_k v_k} \quad (\text{a13})$$

6.2 Files necessary to perform RMC by rmcxas

Core file rmcxas

- rmcxas

is a (compiled) code to perform Reverse Monte Carlo (RMC) analysis of Extended X-ray absorption Fine Structure (EXAFS) spectra and X-ray, neutron or electron scattering or diffraction to obtain quantitative information about the structure of materials.

External codes required (<https://feff.phys.washington.edu/feffproject-feff.html>)

- feff (version 8 or above), generates EXAFS amplitude and phase information (feffijkl.dat files).
- atoms (generates feff.inp and p1.inp (unit cell content) files)

External codes optional

- gnuplot or other software for graphical display of scientific data
- Crystalmaker or other molecular graphic codes (e.g. VESTA)
- atominfo (<https://www.iucr.org/resources/commissions/computing/software-museum>) or other sources for atomic form factor coefficients
- xafsX (<https://xafsx.de>) or any EXAFS data analysis code for pre- and postprocessing

6.3 Auxiliary Files useful to perform RMC by rmcxas and process results of it

Tools for preparation of input to rmcxas (different preliminary development level)

- rebin

Rebinning (diffraction) data to fit the limited assigned memory in rmcxas.

input: rebin.par, and one data set (text file with data in columns)

output: reb.dat

- coord

Generates supercells for rmcxas (rmc.coo type files) using atoms p1.inp output.

input: coord.par

output: crysta.coo, ortho.coo

- cutcylinder

Generates rod-shape like particle models from coord output.

input: crysta.coo

output: cylinder.coo

- distill

Distills coordinates from supercells of rmc.coo type files back into a single unit cell.

input: distill.par, rmc.coo

output: rmc.coo.dis

- double

Doubles the supercell in each direction.

input: rmc.coo

output: rmc.coo.db1

- **extract**

Preprocessing of (standard) diffraction data extracting Bragg reflections and background signal for Rietveld refinement of Cagliotti parameters.

input: `extract.par`, and one diffraction data set (text file with data in columns)

output: `peaks.dat`, `backg.dat`

- **genriepar**

Generates a generic input file for the Rietveld part of the code.

input: `rmc.uc`

output: `rie.par`

- **interface**

Generates complex atomistic models.

input: `crysta.coo`

output: `younameit`

- **mkrmcthe**

Generates `rmc.the` type files from feff output.

input: `feff.inp`, `files.dat`, `feffijhkl.dat`

output: `rmc.the.r`, rename to `rmc.the.i` you may need to change the paths in `rmc.the.i`

- **rancoo**

Substitutes atoms randomly.

input: `rmc.coo`

output: `random.coo`

- **rmc2fef**

Converts type `rmc.coo` type files to coordinates for `feff.inp` without header.

input: `rmc.coo.*`

output: `feff.rmc`

- **sphere**

Generates spherical particle models from `coord` output.

input: `crysta.coo`

output: `sphere.coo`

Tools for analysis of output of `rmcxas`

- **anacon**

Generates Brookhaven Protein Data Base (PDB) coordinate files for input in molecular graphics programs.

input: `anacon.par`

output: `*.pdb`

- **gtot**

Computes the total pair distribution function from the pPDFs in `rmc.pdf` files.

input: `rmc.pdf`

output: `gtot.pdf`

- pdf

Generates pPDFs from `rmc.coo` files including histograms with centered bins in `rmc.his`.

input: `pdf.par`

output: `rmc.his`, `rmc.pdf.pdf`

- pdf2xas

Computes EXAFS from the pPDFs in `rmc.pdf` files.

input: `rmc.pdf`, `rmc.the.i`, EXAFS data file

output: `rmc.spe.sim`

- rmc2opt

Computes optical Fourier transforms from `rmc.spe` files.

input: `rmc.spe.i`, `*.fef`

output: `rmc.dat.dat`, `rmc.rmc.dat`, `rmc.fit.dat`, `rmc.axs.dat`, `rmc.res.dat`,
`rmc.dat.opt`, `rmc.rmc.opt`, `rmc.fit.opt`, `rmc.axs.opt`, `rmc.res.opt`

- rmcana

Analyzes `rmc.pdf` files computing moments of the pPDFs.

input: `rmc.pdf`

output: `rmcana.res`

- transfo

Performs coordinate transformations.

input: `transfo.par`, `rmc.coo.i`

output: `transfo.ort`, `transfo.coo`, `transfo.log`

7 Examples

The following examples do not contain a discussion about the physics, chemistry or materials science aspect of the samples investigated. In some cases this information can be found in the corresponding publications. The examples show and explain for what type of problems and how the `rmcxas` code may be used. The corresponding files can be found in the folder `/rmcxas/examples_and_data`.

7.1 RMC analysis of a single Zr K-edge EXAFS spectrum (m-ZrO₂, 300 K)

(published in M. Winterer, *Reverse Monte Carlo Analysis of EXAFS Spectra of Amorphous and Monoclinic Zirconia*, J. Appl. Phys. **88** (2000), 5635)

This is an example of the most simple use of `rmcxas`, refinement of a single EXAFS spectrum using a single crystalline phase.

```
m-ZrO2 test for analysis of spectroscopy
1 2 1      nphas (<= 2), nscatt in phase 1, nabs in phase 1, 2, ...
1 1 0      nspec (number of spectra <= 3), listsit (absorber to spectrum)
0          ndiff (<=3), diffprobe (x,e,n), compmode ((d)ebye, (s)trf.)
g          imode (input mode for coord.(g)enerate,(i)nput,input&(r)estart)
5.151      alatt (lattice parameter in x) for phase 1, 2, ...
5.207      blatt (lattice parameter in y) for phase 1, 2, ...
5.319      clatt (lattice parameter in z) for phase 1, 2, ...
4          hn (number of unit cells in x) for phase 1, 2, ...
4          kn (number of unit cells in y) for phase 1, 2, ...
4          ln (number of unit cells in z) for phase 1, 2, ...
90.0       alpha (in degrees) for phase 1, 2, ...
99.23      beta (in degrees) for phase 1, 2, ...
90.0,      gamma (in degrees) for phase 1, 2, ...
1.0        fraction of phases for 1, 2 (normalized by program)
2          ntyp (total number of different atom types / scatterers / sites)
0.05       deltar (bin width for radial distributions)
10.0 10.0  rmax (maximum radius for radial distribution)
3.2 1.8 2.3 close(i),i=1,(ntyp*ntyp+ntyp)/2 (clos appr of 2 atoms)
0.1,       drmax (maximum movement by Monte Carlo) for phase 1, 2
.false.    switch for coordination number constraints(from "rmc.con")
768        ncyc (number of cycles to perform)
1          nout (number of cycles after which coordinates etc. are saved)
3          power (power of k-vector)
-5.0       e0shift(j),j=1,nspec (e0-shift for feff, in eV)
1.0        s02(j),j=1,nspec (amplitude reduction factor for feff)
0.000      sig2(j),j=1,nspec (negative:in pdf,positive:in feff,0.0:none)
0.003      errmod(j),j=1,nspec (0.0: err(i)=1)
23,1,2,5,mw_0037to39.mcm
```

Fig. 19: Main control file `rmc.par`

axs.par	mw_0037to39.mcm	rmc.the.1
feff/	rmc.par	rmc.ucc.1

Fig. 20: Folder content before analysis:

axs.par	control file for low frequency signal (not applied here)
feff	folder, contains the feffijlk.dat files
mw_0037to39.mcm	EXAFS data file
rmc.par	main control file for rmcxas
rmc.the.1	file containing paths to feffijlk.dat files for absorber 1
rmc.ucc.1	file containing unit cell content for phase 1

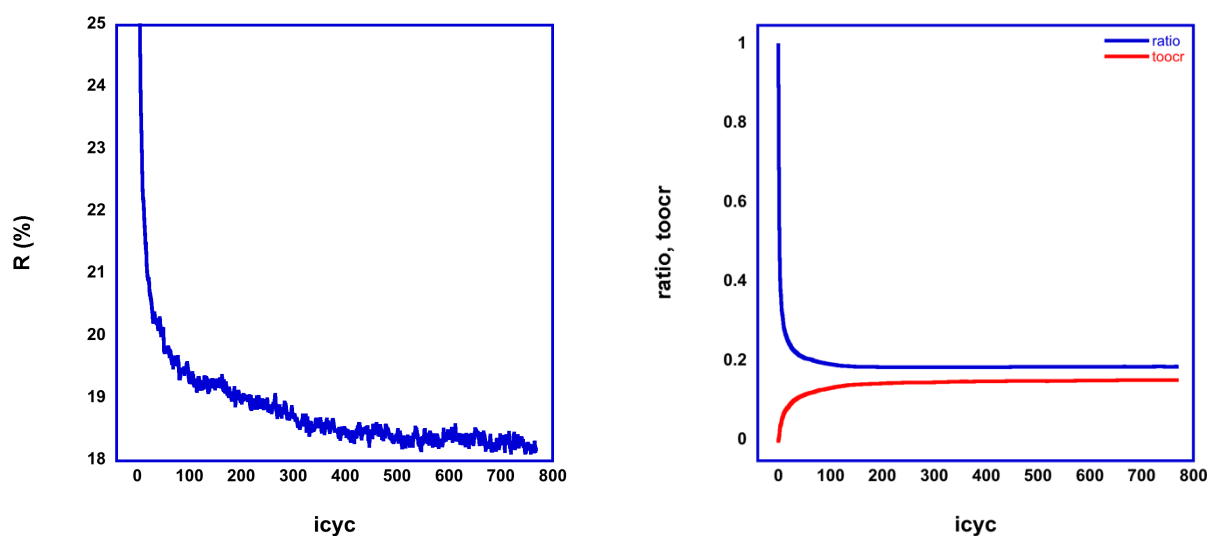


Fig. 21: Performance of rmcxas: refinement index R (left) and acceptance ratio and fraction of RMC steps which are rejected because of hard sphere conditions (right) as a function of RMC cycles.

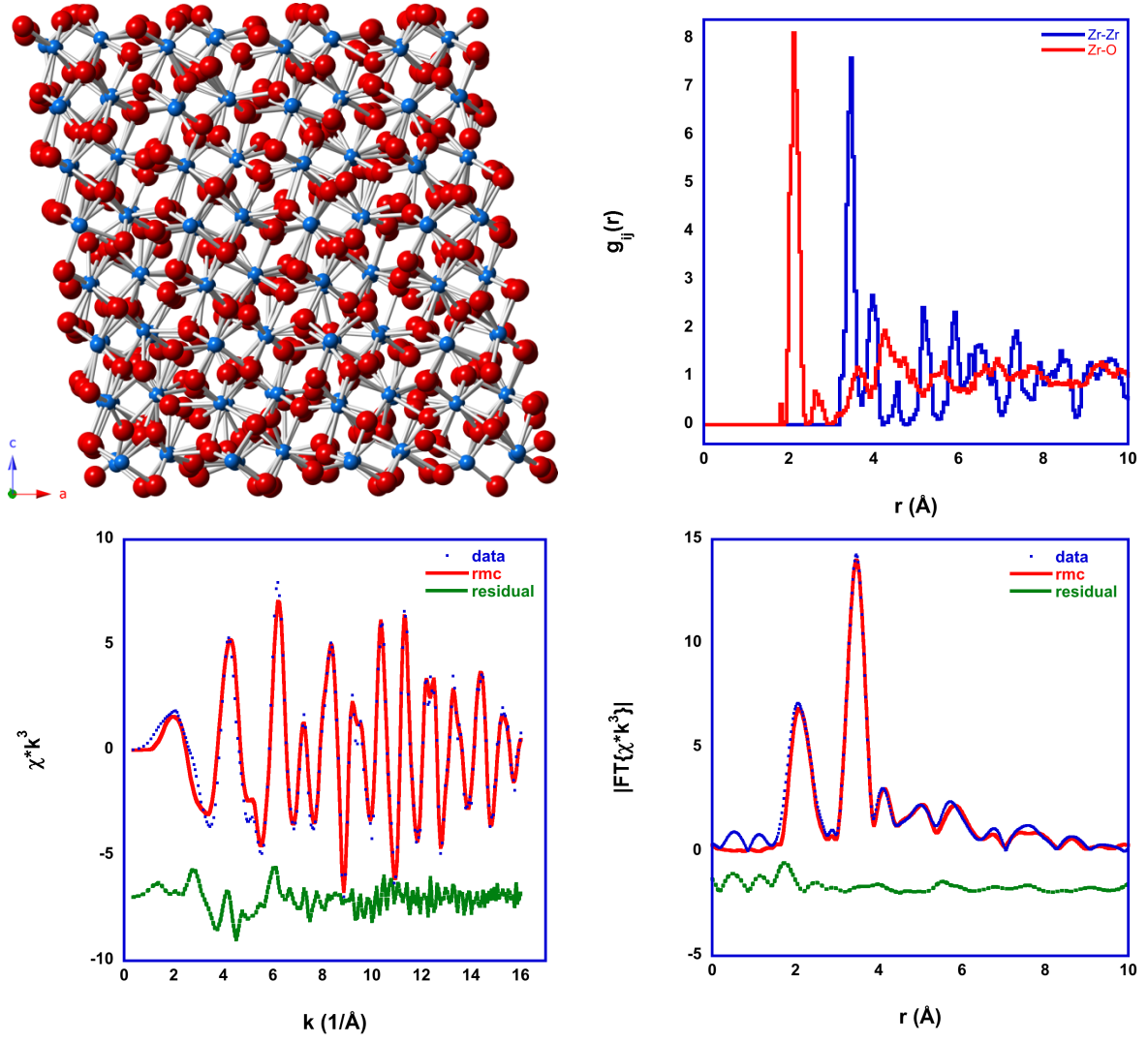


Fig. 22: Atomic configuration (along *b*-axis) (top left), EXAFS spectrum (top right), pPDFs (bottom left) and optical (phase corrected Fourier transform (bottom right) for m-ZrO₂.

7.2 Rietveld refinement of a single XRD data set (m-ZrO₂, 300 K)

This example shows how to perform Rietveld refinement of a X-ray diffractogram using a single crystalline phase.

```
m-ZrO2 Heraeus
1 2 1      nphas (<= 2), nscatt in phase 1, nabs in phase 1, 2, ...
1 1 0      nspec (number of spectra <= 3), listsit (absorber to spectrum)
1 x r 0     ndiff (<=3), diffprobe (x,e,n), compmode ((d)ebye, (s)trf.)
g          imode (input mode for coord.(g)enerate,(i)nput,input&(r)estart)
5.151      alatt (lattice parameter in x) for phase 1, 2, ...
5.212      blatt (lattice parameter in y) for phase 1, 2, ...
5.317      clatt (lattice parameter in z) for phase 1, 2, ...
4 16       hn (number of unit cells in x) for phase 1, 2, ...
4 16       kn (number of unit cells in y) for phase 1, 2, ...
4 10       ln (number of unit cells in z) for phase 1, 2, ...
90.0       alpha (in degrees) for phase 1, 2, ...
99.23      beta (in degrees) for phase 1, 2, ...
90.0       gamma (in degrees) for phase 1, 2, ...
1.0        fraction of phases for 1, 2 (normalized by program)
2          ntyp (total number of different atom types / scatterers / sites)
0.025      deltar (bin width for radial distributions)
10.0,10.0  rmax (maximum radius for radial distribution)
3.2 1.8 2.3 1.0 1.0 1.0 1.0 1.0 1.0 1.0 1.0 close(i),i=1,(ntyp*ntyp+ntyp)/2 (clos
appr of 2 atoms)
0.05,0.025 drmax (maximum movement by Monte Carlo) for phase 1, 2
.false.    switch for coordination number constraints(from "rmc.con")
1          ncy (number of cycles to perform)
1          nout (number of cycles after which coordinates etc. are saved)
3          power (power of k-vector)
-5.0 0.0   e0shift(j),j=1,nspec (e0-shift for feff, in eV)
1.0 1.0    s02(j),j=1,nspec (amplitude reduction factor for feff)
0.000 0.000 sig2(j),j=1,nspec (negative:in pdf,positive:in feff,0.0:none)
0.003 0.003 errmod(j),j=1,nspec (0.0: err(i)=1)
23,1,2,5, mw_0037to39.mcm
-1.54      wavelength (A) or acceleration voltage (V)
0.1        errmod
1,1,2,3,mzro2.xrd.dat
```

Fig. 23: Main control file rmc.par

```
1000 ngmcy
1 1 1 ncycs, ncyce, ncyce
10 gnadjst
1.000000E-02 gacrtio
1.000000E-02 gadjst
1.0 atmov
#
1 16.1936 0.100000E-01 100.000 0.100000E-01 0 0.000000 0.000000 intensity_scale
2 -0.676966E-02 -0.100000 0.100000 0.100000E-04 0 0.000000 0.000000 offset
3 -0.310136E-01 -0.100000 0.100000 0.100000E-03 0 0.000000 0.000000 sample
4 0.461980E-01 -0.100000 0.100000 0.100000E-03 0 0.000000 0.000000 transparency
5 0.773000E-02 0.000000 0.100000 0.000000 0 0.000000 0.000000 u_cagliotti
6 -0.483000E-02 -0.100000 0.100000 0.000000 0 0.000000 0.000000 v_cagliotti
7 0.383000E-02 -0.100000 0.100000 0.000000 0 0.000000 0.000000 w_cagliotti
8 28.2216 -100.000 100.000 0.100000E-01 0 0.000000 0.000000 backgr0
9 7.48759 -100.000 120.000 0.100000E-01 0 0.000000 0.000000 backgr1
10 -2.10150 -100.000 120.000 0.100000E-01 0 0.000000 0.000000 backgr2
```

11	0.000000	0.100000E-01	120.000	0.000000	0	0.000000	0.000000	backgr3
12	0.000000	0.100000E-01	120.000	0.000000	0	0.000000	0.000000	backgr4
13	0.000000	0.100000E-01	120.000	0.000000	0	0.000000	0.000000	backgr5
14	0.000000	0.100000E-01	120.000	0.000000	0	0.000000	0.000000	backgr6
15	0.000000	0.100000E-01	120.000	0.000000	0	0.000000	0.000000	backgr7
16	0.000000	0.100000E-01	120.000	0.000000	0	0.000000	0.000000	backgr8
17	0.000000	0.100000E-01	120.000	0.000000	0	0.000000	0.000000	backgr9
18	0.000000	0.100000E-01	120.000	0.000000	0	0.000000	0.000000	backgr10
19	0.000000	0.100000E-01	120.000	0.000000	0	0.000000	0.000000	backgr11
20	30.0000	0.100000E-01	120.000	0.000000	0	0.000000	0.000000	backgrposition
21	1.00000	0.100000E-03	1.00000	0.000000	0	0.000000	0.000000	phasefraction
22	1389.36	1.00000	100000.	1.00000	0	0.000000	0.000000	columnlength(A)
23	0.393229E-02	0.100000E-05	0.500000E-01	0.100000E-04	0	0.000000	0.000000	microstrain
24	5.14886	5.00000	5.50000	0.100000E-05	0	0.000000	0.000000	alatt(A)
25	5.20394	5.00000	5.50000	0.100000E-05	0	0.000000	0.000000	blatt(A)
26	5.32317	5.00000	5.50000	0.100000E-05	0	0.000000	0.000000	clatt(A)
27	90.0000	0.000000	0.000000	0.000000	0	0.000000	0.000000	alphad(deg)
28	99.1502	90.0000	120.000	0.100000E-02	0	0.000000	0.000000	betad(deg)
29	90.0000	0.000000	0.000000	0.000000	0	0.000000	0.000000	gammd(deg)
30	12.0000	0.000000	0.000000	0.000000	0	0.000000	0.000000	nsit1
31	1.00000	0.000000	0.000000	0.000000	0	0.000000	0.000000	atomtype1
32	1.00000	0.000000	0.000000	0.000000	0	0.000000	0.000000	occ1
33	0.275173	0.000000	1.00000	0.100000E-03	0	0.000000	0.000000	xuc1
34	0.392672E-01	0.000000	1.00000	0.100000E-03	0	0.000000	0.000000	yuc1
35	0.208896	0.000000	1.00000	0.100000E-03	0	0.000000	0.000000	zuc1
36	0.600000E-02	0.100000E-02	0.100000	0.100000E-05	0	0.000000	0.000000	umsq1
37	2.00000	0.000000	0.000000	0.000000	0	0.000000	0.000000	atomtype2
38	1.00000	0.000000	1.00000	0.000000	0	0.000000	0.000000	occ2
39	0.728464E-01	0.000000	1.00000	0.100000E-03	0	0.000000	0.000000	xuc2
40	0.329758	0.000000	1.00000	0.100000E-03	0	0.000000	0.000000	yuc2
41	0.348312	0.000000	1.00000	0.100000E-03	0	0.000000	0.000000	zuc2
42	0.600000E-02	0.100000E-02	0.100000	0.000000	36	1.00000	0.000000	umsq2
43	2.00000	0.100000E-02	0.000000	0.000000	0	0.000000	0.000000	atomtype3
44	1.00000	0.000000	0.000000	0.000000	0	0.000000	0.000000	occ3
45	0.450536	0.000000	1.00000	0.100000E-03	0	0.000000	0.000000	xuc3
46	0.758720	0.000000	1.00000	0.100000E-03	0	0.000000	0.000000	yuc3
47	0.478746	0.000000	1.00000	0.100000E-03	0	0.000000	0.000000	zuc3
48	0.600000E-02	0.100000E-02	0.100000	0.000000	36	1.00000	0.000000	umsq3
49	1.00000	0.000000	0.000000	0.000000	0	0.000000	0.000000	atomtype4
50	1.00000	0.000000	0.000000	0.000000	0	0.000000	0.000000	occ4
51	-0.275173	0.000000	1.00000	0.000000	33	-1.00000	0.000000	xuc4
52	0.539267	0.000000	1.00000	0.000000	34	1.00000	0.500000	yuc4
53	0.291104	0.000000	1.00000	0.000000	35	-1.00000	0.500000	zuc4
54	0.600000E-02	0.100000E-02	0.100000	0.000000	36	1.00000	0.000000	umsq4
55	2.00000	0.000000	0.000000	0.000000	0	0.000000	0.000000	atomtype5
56	1.00000	0.000000	0.000000	0.000000	0	0.000000	0.000000	occ5
57	-0.728464E-01	0.000000	1.00000	0.000000	39	-1.00000	0.000000	xuc5
58	0.829758	0.000000	1.00000	0.000000	40	1.00000	0.500000	yuc5
59	0.151688	0.000000	1.00000	0.000000	41	-1.00000	0.500000	zuc5
60	0.600000E-02	0.100000E-02	0.100000	0.000000	36	1.00000	0.000000	umsq5
61	2.00000	0.000000	0.000000	0.000000	0	0.000000	0.000000	atomtype6
62	1.00000	0.000000	0.000000	0.000000	0	0.000000	0.000000	occ6
63	-0.450536	0.000000	1.00000	0.000000	45	-1.00000	0.000000	xuc6
64	1.25872	0.000000	1.00000	0.000000	46	1.00000	0.500000	yuc6
65	0.212541E-01	0.000000	1.00000	0.000000	47	-1.00000	0.500000	zuc6
66	0.600000E-02	0.100000E-02	0.100000	0.000000	36	1.00000	0.000000	umsq6
67	1.00000	0.000000	0.000000	0.000000	0	0.000000	0.000000	atomtype7
68	1.00000	0.000000	0.000000	0.000000	0	0.000000	0.000000	occ7
69	-0.275173	0.000000	1.00000	0.000000	33	-1.00000	0.000000	xuc7
70	-0.392672E-01	0.000000	1.00000	0.000000	34	-1.00000	0.000000	yuc7
71	-0.208896	0.000000	1.00000	0.000000	35	-1.00000	0.000000	zuc7
72	0.600000E-02	0.100000E-02	0.100000	0.000000	36	1.00000	0.000000	umsq7
73	2.00000	0.000000	0.000000	0.000000	0	0.000000	0.000000	atomtype8
74	1.00000	0.000000	0.000000	0.000000	0	0.000000	0.000000	occ8
75	-0.728464E-01	0.000000	1.00000	0.000000	39	-1.00000	0.000000	xuc8
76	-0.329758	0.000000	1.00000	0.000000	40	-1.00000	0.000000	yuc8
77	-0.348312	0.000000	1.00000	0.000000	41	-1.00000	0.000000	zuc8
78	0.600000E-02	0.100000E-02	0.100000	0.000000	36	1.00000	0.000000	umsq8
79	2.00000	0.000000	0.000000	0.000000	0	0.000000	0.000000	atomtype9
80	1.00000	0.000000	0.000000	0.000000	0	0.000000	0.000000	occ9
81	-0.450536	0.000000	1.00000	0.000000	45	-1.00000	0.000000	xuc9
82	-0.758720	0.000000	1.00000	0.000000	46	-1.00000	0.000000	yuc9
83	-0.478746	0.000000	1.00000	0.000000	47	-1.00000	0.000000	zuc9
84	0.600000E-02	0.100000E-02	0.100000	0.000000	36	1.00000	0.000000	umsq9
85	1.00000	0.000000	0.000000	0.000000	0	0.000000	0.000000	atomtype10
86	1.00000	0.000000	0.000000	0.000000	0	0.000000	0.000000	occ10
87	0.275173	0.000000	1.00000	0.000000	33	1.00000	0.000000	xuc10
88	0.460733	0.000000	1.00000	0.000000	34	-1.00000	0.500000	yuc10
89	0.708896	0.000000	1.00000	0.000000	35	1.00000	0.500000	zuc10
90	0.600000E-02	0.100000E-02	0.100000	0.000000	36	1.00000	0.000000	umsq10
91	2.00000	0.000000	0.000000	0.000000	0	0.000000	0.000000	atomtype11
92	1.00000	0.000000	0.000000	0.000000	0	0.000000	0.000000	occ11

93	0.728464E-01	0.000000	1.00000	0.000000	39	1.00000	0.000000	xuc11
94	0.170242	0.000000	1.00000	0.000000	40	-1.00000	0.500000	yuc11
95	0.848312	0.000000	1.00000	0.000000	41	1.00000	0.500000	zuc11
96	0.600000E-02	0.100000E-02	0.100000	0.000000	36	1.00000	0.000000	umsq11
97	2.00000	0.000000	0.000000	0.000000	0	0.000000	0.000000	atomtype12
98	1.00000	0.000000	0.000000	0.000000	0	0.000000	0.000000	occ12
99	0.450536	0.000000	1.00000	0.000000	45	1.00000	0.000000	xuc12
100	-0.258720	0.000000	1.00000	0.000000	46	-1.00000	0.500000	yuc12
101	0.978746	0.000000	1.00000	0.000000	47	1.00000	0.500000	zuc12
102	0.600000E-02	0.100000E-02	0.100000	0.000000	36	1.00000	0.000000	umsq12

Fig. 24: Rietveld control file rie.par

Table 1: Rietveld results and comparison to published data

Instrument

Variable	value (error)
scale	16.15(2)
2θ offset	$-6.71(2) \cdot 10^{-3}$
sample displacement	$-3.101(1) \cdot 10^{-2}$
sample transparency	$4.600(6) \cdot 10^{-2}$
b_0	28.14(3)
b_1	6.4((4)
b_2	-1.7(1)

Microstructure monoclinic

d (nm)	138.7(2)	200(30)
ε (%)	0.393(8)	0.24(1)

(Winterer 2002, fullprof refinement)

Crystal Structure

a (Å)	5.149(2)	5.1451(3)
b (Å)	5.204(4)	5.2023(4)
c (Å)	5.323(3)	5.3219(4)
β (°)	99.15(4)	99.15(3)

fractional coordinates

$x(\text{Zr})$	0.2741 (-)	0.2760(5)
$y(\text{Zr})$	0.00393(2)	0.0401(4)
$z(\text{Zr})$	0.20889(6)	0.2091(4)

$x(\text{O}_1)$	0.07279(9)	0.072(3)
$y(\text{O}_1)$	0.3297(2)	0.333(2)
$z(\text{O}_1)$	0.3485(2)	0.347(2)

$x(\text{O}_2)$	0.4503(2)	0.449(3)
$y(\text{O}_2)$	0.7587(2)	0.758(2)
$z(\text{O}_2)$	0.4786(2)	0.476(3)

u^2 (Å ²)	$5.1(3) \cdot 10^{-3}$	$5.183(5) \cdot 10^{-3}$
-------------------------	------------------------	--------------------------

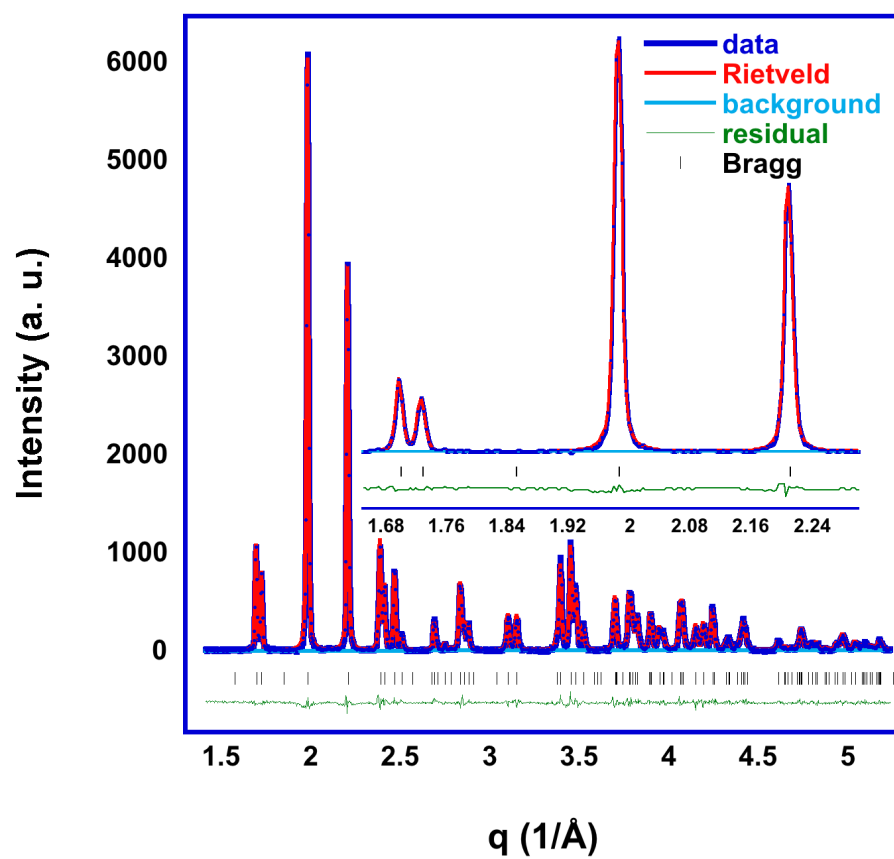


Fig. 25: XRD data and Rietveld refinement ($R = 7.08\%$)

7.3 Coupled RMC of Zr K-edge EXAFS and Rietveld refinement of XRD data set (m-ZrO₂, 300 K)

(unpublished, based on data published in M. Winterer, Nanocrystalline Ceramics – Synthesis and Structure, Springer, Heidelberg 2002, Springer Series in Materials Science, Volume 53, ISBN 3-540-43433-X)

This example shows how to couple RMC analysis of EXAFS and Rietveld refinement of XRD data.

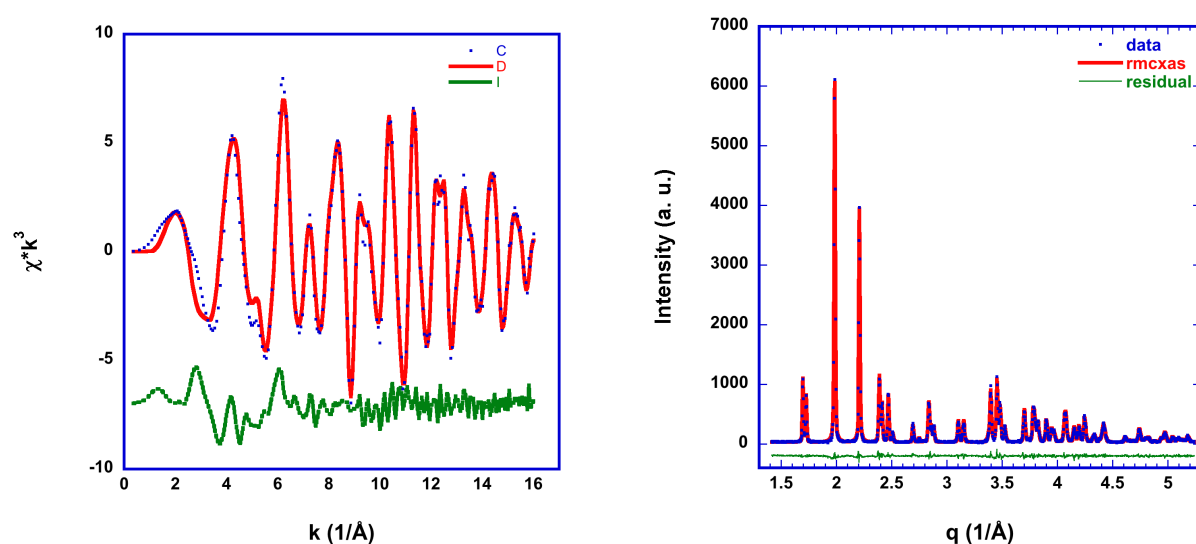


Fig. 26: Coupled refinement of Zr-K-edge EXAFS spectrum ($R = 18.9\%$) and XRD ($R = 6.81\%$)

Table 1: Results from pPDFs after RMC refinement of EXAFS coupled to XRD

shell	range (Å)	refined (RMC)			initial	
		$N \propto p_0$ ()	$p_1 = \langle r \rangle$ (Å)	$p_2 = \sigma^2$ (10^{-3} Å^2)	$N \propto p_0$ ()	$p_1 = \langle r \rangle$ (Å)
Zr-O	1.9 – 2.5	6.7 (13)	2.15 (2)	9 (2)	7.0	2.15
Zr-Zr	3.0 – 3.7	7.0 (12)	3.45 (2)	8 (2)	7.0	3.46
	3.7 – 4.3	4.0 (8)	3.96 (2)	11 (3)	4.0	3.96
	4.3 – 4.8	1.0 (2)	4.53 (2)	7 (2)	1.0	4.54

Table 1: Rietveld results and comparison to published data**Instrument**

Variable	value (error)
scale	15.8 (2)
2θ offset	$-1.191(8) \cdot 10^{-2}$
sample displacement	$-2.540(1) \cdot 10^{-2}$
sample transparency	$5.4 \cdot 10^{-2}$
b_0	28.4(8)
b_1	-1.8(8)
b_2	1.9(5)

**Microstructure
monoclinic****(Winterer 2002, fullprof refinement)**

d (nm)	160(90)	200(30)
ε (%)	0.45(4)	0.24(1)

Crystal Structure

a (Å)	5.149(3)	5.1451(3)
b (Å)	5.204(3)	5.2023(4)
c (Å)	5.324(5)	5.3219(4)
β (°)	99.15(3)	99.15(3)

fractional coordinates

$x(\text{Zr})$	0.2750(3)	0.2760(5)
$y(\text{Zr})$	0.0039(4)	0.0401(4)
$z(\text{Zr})$	0.2090(3)	0.2091(4)

$x(\text{O}_1)$	0.0724(7)	0.072(3)
$y(\text{O}_1)$	0.3293(7)	0.333(2)
$z(\text{O}_1)$	0.3490(4)	0.347(2)

$x(\text{O}_2)$	0.4494(5)	0.449(3)
$y(\text{O}_2)$	0.7587(4)	0.758(2)
$z(\text{O}_2)$	0.4779(10)	0.476(3)

u^2 (Å ²)	$1.0(6) \cdot 10^{-3}$	$5.183(5) \cdot 10^{-3}$
-------------------------	------------------------	--------------------------

7.4 Coupled RMC of Zr K-edge EXAFS and Rietveld refinement of XRD data set (Al doped t-ZrO₂, 300 K)

(unpublished, based on data published in M. Winterer, Nanocrystalline Ceramics – Synthesis and Structure, Springer, Heidelberg 2002, Springer Series in Materials Science, Volume 53, ISBN 3-540-43433-X)

This example shows how to couple RMC analysis of EXAFS and Rietveld refinement of XRD data when one site (Zr) is substituted by another element (Al). This may be used for doped systems or solid solutions.

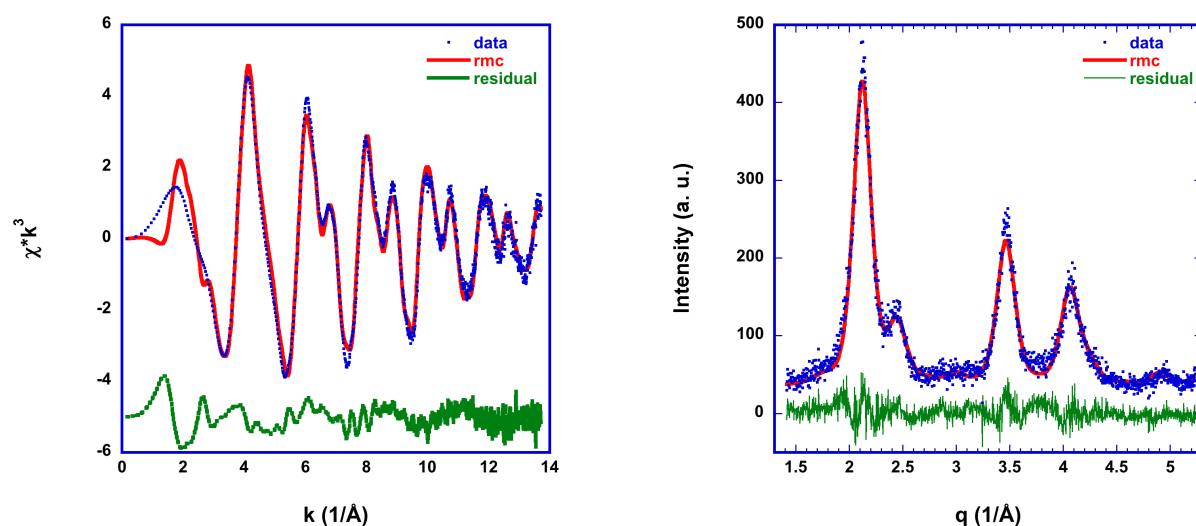


Fig. 27: Coupled refinement of Zr-K-edge EXAFS spectrum ($R = 17.7\%$) and XRD ($R = 9.96\%$)

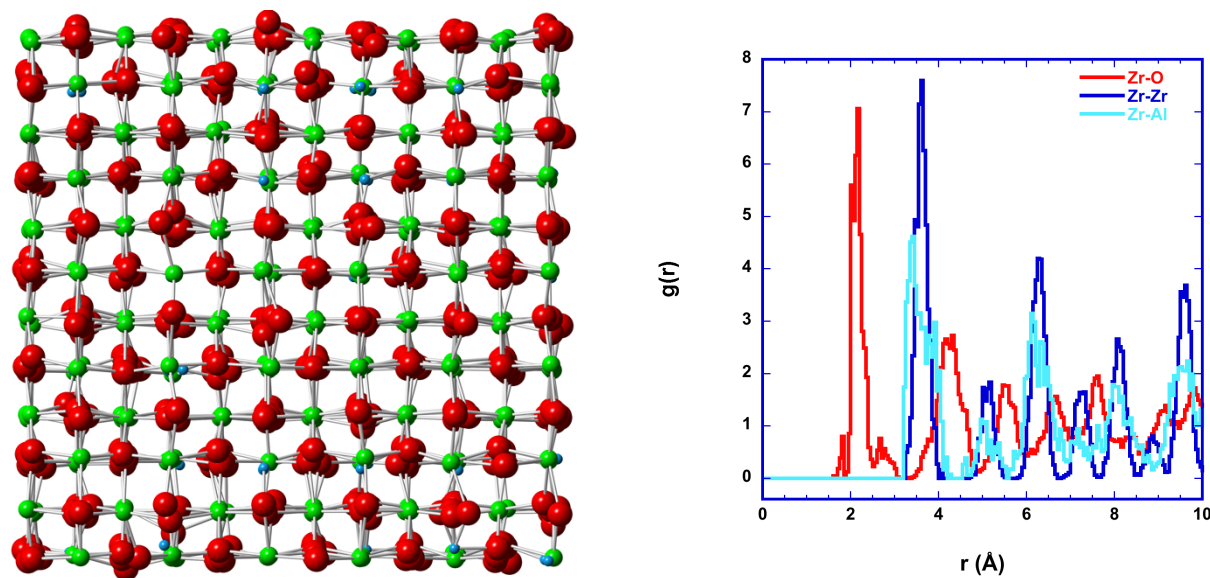


Fig. 28: Atomic configuration (O: red, Zr: green, Al: blue, a - b projection) after refinement and pPDFs.

Table 1: Results from pPDFs from RMC refinement of EXAFS coupled to XRD

shell	range (Å)	refined (RMC)		
		$N \propto p_0$ ()	$p_1 = \langle r \rangle$ (Å)	$p_2 = \sigma^2$ (10^{-3} Å^2)
Zr-O	1.9 – 2.5	6.6 (17)	2.17 (3)	13 (5)
Zr-Zr	3.0 – 4.5	10.0 (16)	3.62 (3)	19 (5)
Zr-Al	3.0 – 4.5	2.0 (3)	3.60 (4)	61 (11)

Table 1: Rietveld results and comparison to published data**Instrument****Variable** **value (error)**

scale	9.99 (12)
b_0	33.3(2)
b_1	0.003(18)
b_2	0.003(8)

**Microstructure
monoclinic****(Winterer 2002, fullprof refinement)**

d (nm)	4.21(2)	2.5(1)
ε (%)	0.15(2)	0

Crystal Structure

a (Å)	3.611(2)	3.604(4)
c (Å)	5.174(2)	5.18(1)

fractional coordinates

$o(\text{Zr}_1)$	0.708(16)	
$u^2(\text{Zr}_1) (\text{Å}^2)$	$19(5) \cdot 10^{-3}$	$19(3) \cdot 10^{-3}$
$u^2(\text{Al}) (\text{Å}^2)$	$61(11) \cdot 10^{-3}$	$19(3) \cdot 10^{-3}$
$z(\text{O}_1)$	0.548(5)	0.545(5)
$u^2(\text{O}_1) (\text{Å}^2)$	$13(5) \cdot 10^{-3}$	$34(6) \cdot 10^{-3}$

7.5 Coupled RMC of Zr K-edge EXAFS and Rietveld of XRD for two phases in nano-ZrO₂ (m-ZrO₂, and t-ZrO₂, 300 K) (unpublished)

This example shows how to couple RMC analysis of EXAFS and Rietveld refinement of XRD data when the sample contains two phases.

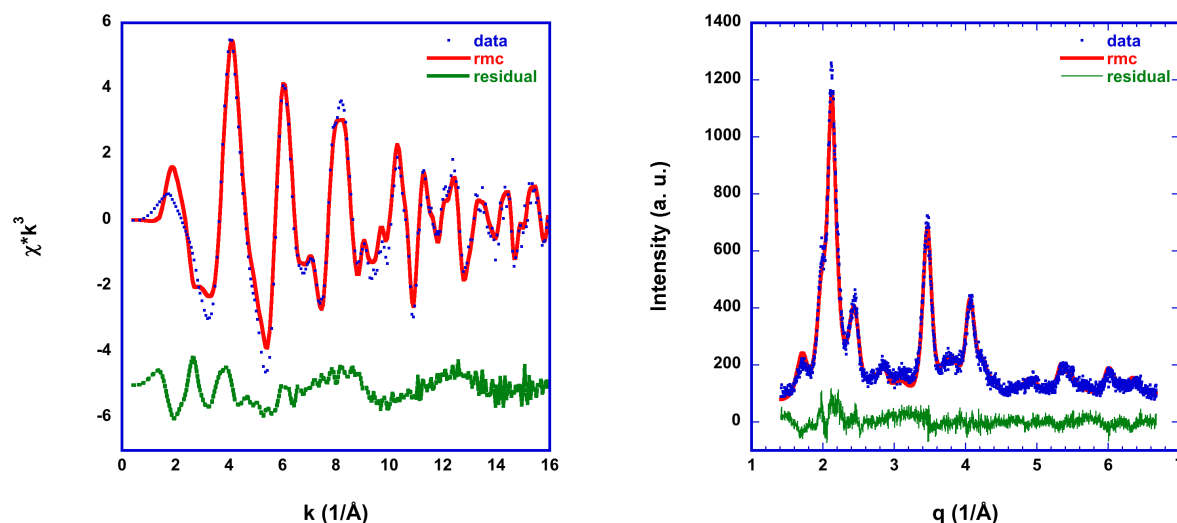


Fig. 29: Coupled refinement of Zr-K-edge EXAFS spectrum ($R = 24.7\%$) and XRD ($R = 7.76\%$)

Table 1: Rietveld results

Microstructure

	monoclinic	tetragonal
phase fraction (%)	56	44
d (nm)	5.29(6)	7.30(9)
ε (%)	1.0(14)	1.0(3)

Crystal Structure

a (Å)	5.142(3)	3.6390(10)
b (Å)	5.206(1)	
c (Å)	5.323(5)	5.061(4)
β (°)	98.49(6)	

7.6 Coupled RMC of Zr K-edge EXAFS and Rietveld of XRD and neutron diffraction: m-ZrO₂

(unpublished, based on data published in M. Winterer, B. Delaplane, R. McGreevy, *X-Ray Diffraction, Neutron Scattering and EXAFS Spectroscopy of Monoclinic Zirconia: Analysis by Rietveld Refinement and Reverse Monte Carlo Simulations*, J. Appl. Cryst. **35** (2002), 434)

This example shows how to couple RMC analysis of EXAFS and Rietveld refinement of X-ray and neutron diffraction data.

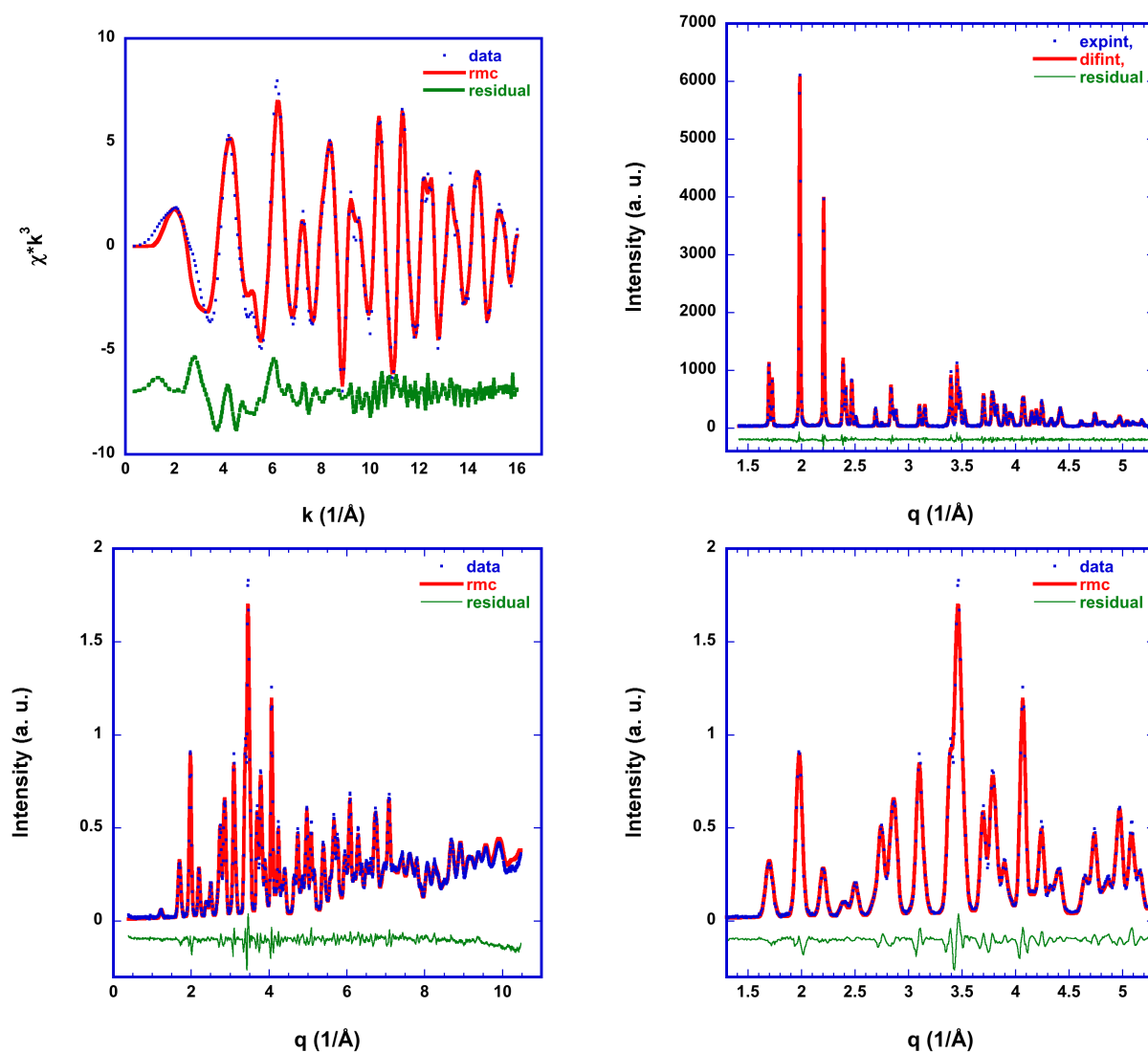


Fig. 30: Coupled refinement of Zr-K-edge EXAFS spectrum ($R = 18.6\%$), X-ray ($R = 7.02\%$) (top row) and neutron diffraction data ($R = 6.18\%$) (bottom row; right enlarged to the same q -range as XRD)

7.7 Simultaneous RMC of EXAFS and neutron scattering $S(q)$: m-ZrO₂

(published in M. Winterer, B. Delaplane, R. McGreevy, *X-Ray Diffraction, Neutron Scattering and EXAFS Spectroscopy of Monoclinic Zirconia: Analysis by Rietveld Refinement and Reverse Monte Carlo Simulations*, J. Appl. Cryst. **35** (2002), 434)

This example shows how to simultaneously perform RMC analysis of EXAFS and neutron scattering data.

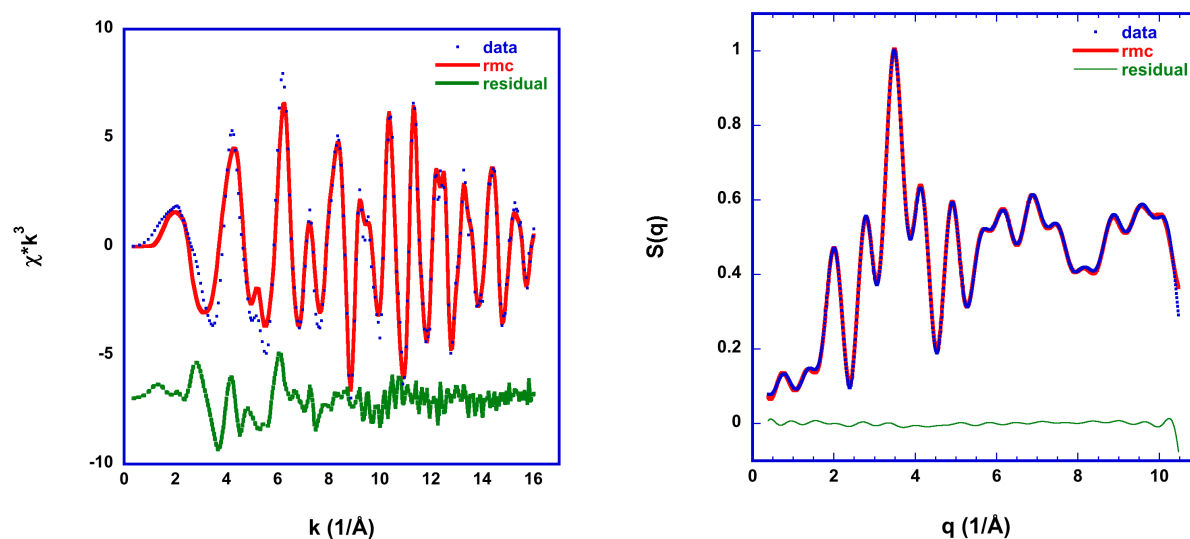


Fig. 31: Simultaneous refinement of Zr-K-edge EXAFS spectrum ($R = 21.9\%$), X-ray ($R = 7.02\%$) (top row) and neutron diffraction structure factor (convoluted to fit simulation box) ($R = 3.08\%$) (bottom row)

7.8 Simultaneous RMC of Co and Zn K-edge EXAFS: Co doped ZnO

(published in R. Djenadic, G. Akgul, K. Attenkofer, and M. Winterer, *Chemical Vapor Synthesis and Structural Characterization of Nanocrystalline $\text{Zn}_{1-x}\text{Co}_x\text{O}$ ($x = 0-0.50$) Particles by X-ray Diffraction and X-ray Absorption Spectroscopy*, J. Phys. Chem. **114** (2010), 9207-9215), see also R. Djenadic and M. Winterer, chapter 2, *Chemical Vapor Synthesis of Nanocrystalline Oxides*, in Axel Lorke, Markus Winterer, Roland Schmechel, und Christof Schulz (eds.), *Nanoparticles from the Gas Phase – Formation, Structure, Properties*, Springer Berlin **2012**, ISBN 978-3-642-28546-2

This example shows how to simultaneously perform RMC analysis of two EXAFS spectra for a solid solution.

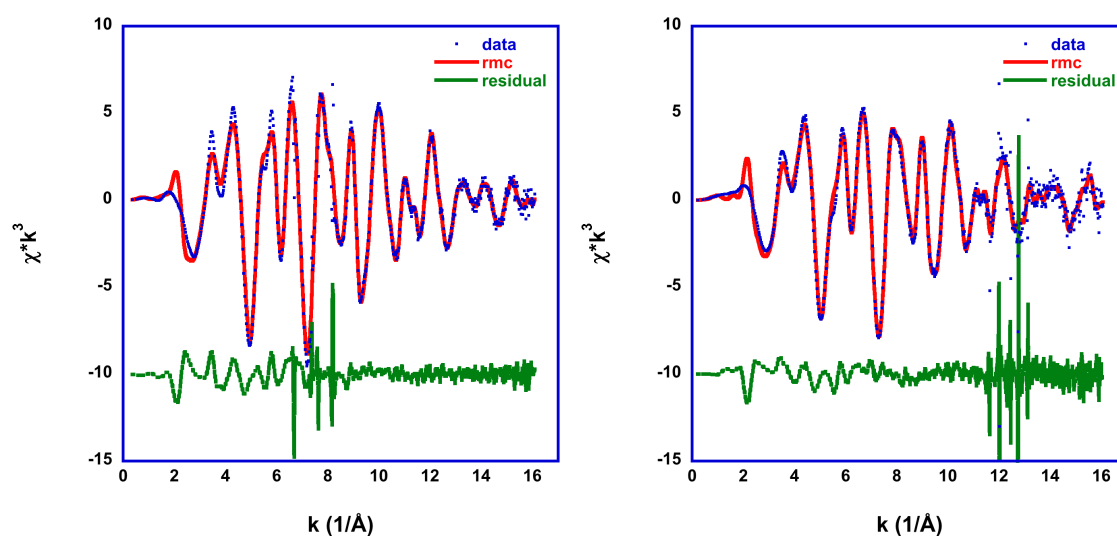


Fig. 32: Simultaneous refinement of Zn (left) and Co K-edge (right) EXAFS spectra ($R = 17.9\%$) ($R = 23.1\%$) for a solid solution of CoO in ZnO. (25% CoO). The sharp peaks in the residual are due to monochromator glitches in the data. The remaining residual is dominated by multiple scattering contributions not refined and by noise.

7.9 Simultaneous RMC of Co and Fe K-edge EXAFS: CoFe₂O₄

(published in J. Geiss, T. Falk, S. Ognjanovic, S. Anke, B. Peng, M. Muhler, and M. Winterer, *Atom Pair Frequencies as a Quantitative Structure–Activity Relationship for Catalytic 2-Propanol Oxidation over Nanocrystalline Cobalt–Iron–Spinel*, J. Phys. Chem. C **126** (2022) 10346–10358)

This example shows how to simultaneously perform RMC analysis of two EXAFS spectra of a complex oxide.

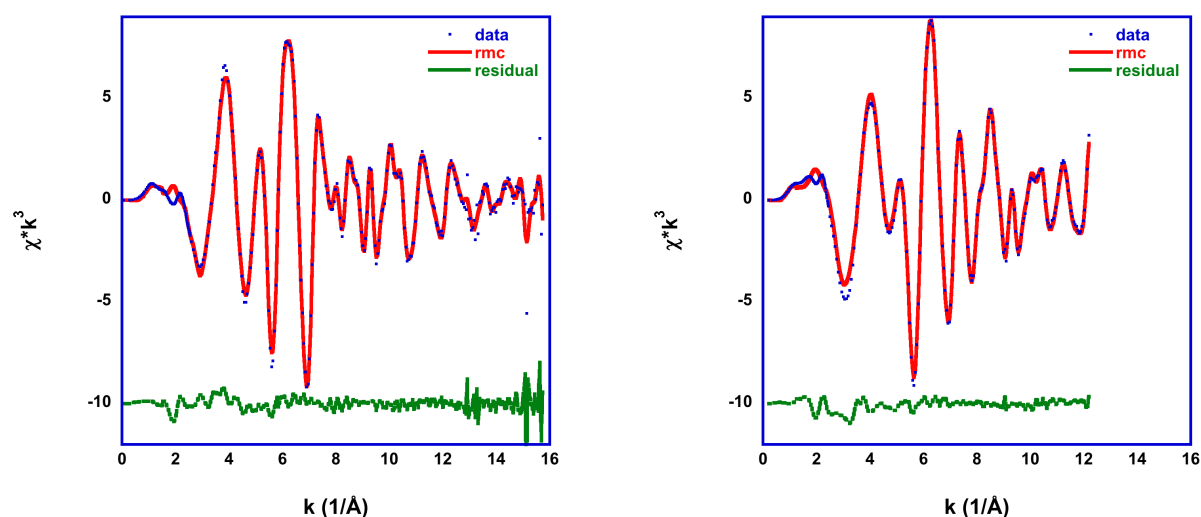


Fig. 33: Simultaneous refinement of Co (left) and Fe (right) K-edge EXAFS spectra ($R = 15.0\%$) ($R = 10.1\%$) for the complex oxide (spinel) CoFe₂O₄.

7.10 Simultaneous RMC of EXAFS and scattering via DSE: SnO₂

(published in V. Mackert, T. Winter, S. Jackson, R. Kalia, A. Levish, S. Lukic, J. Geiss, and M. Winterer, *Very Small Nanocrystalline Tin Dioxide Particles: Local-, Crystal-, and Micro-Structure*, J. Phys. Chem. C **127** (2023) 17389–17405) see also Winterer 2025.

This example shows how to simultaneously perform RMC analysis of an EXAFS spectrum and X-ray scattering data of nanoparticles using the Debye Scattering Equation.

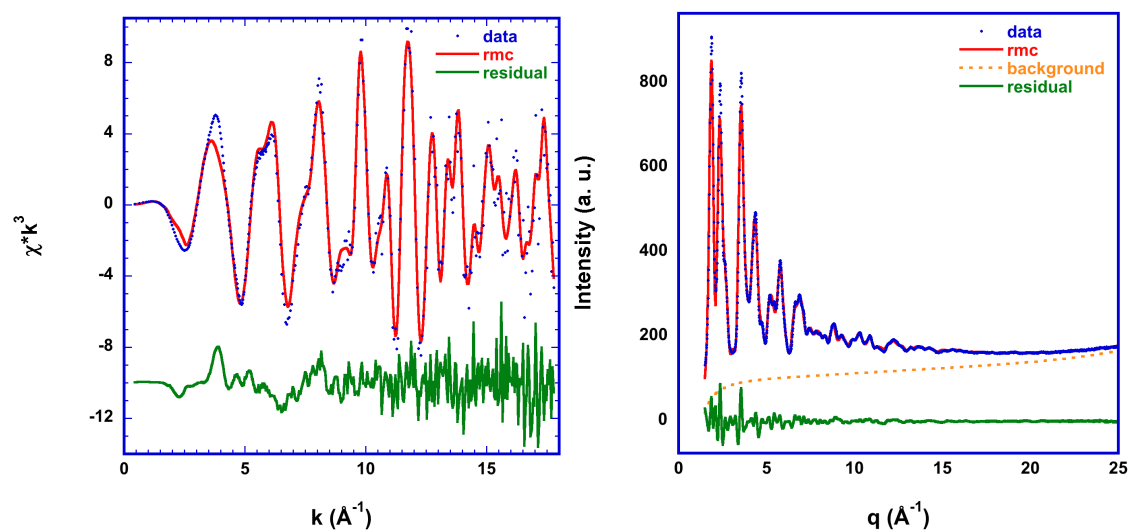


Fig. 34: Simultaneous refinement of Sn-K-edge EXAFS spectrum ($R = 24.0\%$) and WAXS data ($R = 2.09\%$)